DOI: 10.1002/chem.200700663

Xylogranatins F–R: Antifeedants from the Chinese Mangrove, *Xylocarpus granatum*, A New Biogenetic Pathway to Tetranortriterpenoids

Jun Wu,*[a] Si Zhang,[a] Torsten Bruhn,[b] Qiang Xiao,[c] Haixin Ding,[c] and Gerhard Bringmann*[b]

Dedicated to Professor Dr. Peter Welzel on the occasion of his 70th birthday

Abstract: Thirteen limonoids with a new carbon skeleton, the xylogranatins F–R (**1**–**13**), have been isolated from the seeds of a Chinese mangrove, *Xylocarpus granatum*; two recently reported compounds, xylogranatins C and D were also isolated. Their structures were elucidated on the basis of spectroscopic data and chemical methods. The absolute configurations of these compounds were determined by using the modified Mosher MTPA ester method and by quantum chemical circular dichroism (CD) calculations. Xylogranatins F–Q are the first aromatic B-ring limonoids found in nature. They belong to two substructural classes, of which one (**1**–**3**) contains a pyridine ring while the other one (**4**–**12**) contains a central furan core. Xylogranatins C and R can be considered to be key biosynthetic intermediates, while xylogranatin D, the only limonoid found so far with a carbon skeleton that conatains a C_{30}–C_9 linkage, is apparently an artifact. The structures of these compounds suggest a new biogenetic pathway to tetranortriterpenoids. Xylogranatins F, G and R were found to exhibit marked antifeedant activity against the third instar larvae of *Mythimna separata* (Walker) at a concentration of 1 mg mL^{-1}. The most potent compound tested was xylogranatin G. Its AFC_{50} (concentration for 50% antifeedant activity) values at the exposure times of 24 and 48 h were 0.31 and 0.30 mg mL^{-1}, respectively.

Keywords: antifeedant activity · biosynthesis · configuration determination · natural products · xylogranatins

Introduction

Limonoids, which have been found to date only in plants of the order Rutales, are tetranortriterpenoids with a β-furyl ring substituent located at C17 that is derived from a precursor with a 4,4,8-trimethyl-17-furanylsteroid skeleton. They are classified by the four-ring structure in the intact triterpene core unit, and these are usually oxidized and designated as A, B, C and D. The mangrove, *Xylocarpus granatum*, is known to produce antifeedant limonoids, especially phragmalins and mexicanolides. Previous investigations on the seeds of two Meliaceae plants, the mangroves, *X. granatum* and *X. moluccensis*, uncovered one obacunol, two phragmalins, three andirobins, and 14 mexicanolides, including the xyloccensins A–K.[1–5] During the course of our search for potential lead structures from Chinese tropical mangrove plants, we have reported the isolation and identification of a mixture of butyrospermol fatty acid esters,[6] eleven mexicanolides and 13 phragmalins, named xyloccensins L–Z[7–15] and xylogranatins A–E,[16–17] from the stem bark and fruit of a Chinese mangrove *X. granatum*. Five phragmalins, four of which were the same as reported by us earlier,[9] have been obtained from the stem bark of the same plant.[18] On the other hand, two mexicanolides from the fruit of *X. moluccensis*,[19] although structurally different from our xyloccen-

[a] Dr. J. Wu, Prof. S. Zhang
Guangdong Key Laboratory of Marine Materia Medica
South China Sea Institute of Oceanology
Chinese Academy of Sciences, 164 West Xingang Road
510301 Guangzhou (P.R. China)
Fax: (+86) 20-8445-1672
E-mail: wwujun2003@yahoo.com

[b] Dr. T. Bruhn, Prof. Dr. G. Bringmann
Institute for Organic Chemistry, University Würzburg
Am Hubland, 97074 Würzburg (Germany)
Fax: (+49) 931-888-4755
E-mail: bringmann@chemie.uni-wuerzburg.de

[c] Dr. Q. Xiao, H. Ding
Institute of Organic Chemistry
Jiangxi Science & Technology Normal University
330013 Nanchang (P.R. China)

Supporting information for this article is available on the WWW under http://www.chemeurj.org/ or from the author.

sins X (including xyloccensins X_1 and X_2) and Y,[13,14] were, nonetheless, given the same names, xyloccensins X and Y. Furthermore, four unusual 9,10-*seco*-limonoids, named xylogranatins A–D,[20] of which two had previously been isolated by us, have been isolated from the seeds of the same plant. In the current paper, we present the isolation and characterization of thirteen limonoids with new carbon skeletons, xylogranatins F–R (**1**–**13**; Scheme 1), from the seeds

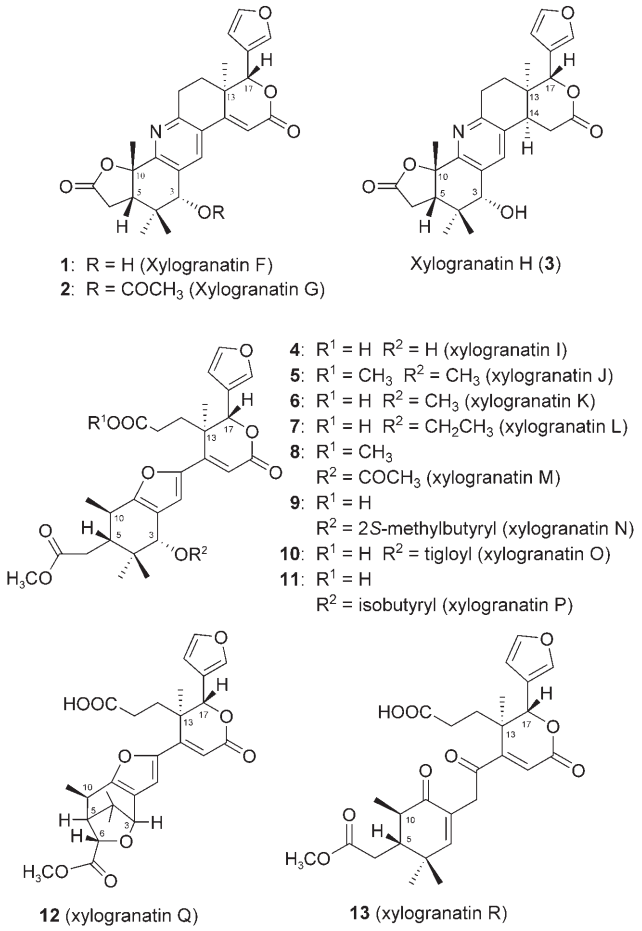

Scheme 1. The xylogranatins F-R (**1**–**13**) isolated from *X. granatum*.

of *X. granatum*. Their constitutions and relative configurations were elucidated by spectroscopic and chemical methods. The absolute configurations of these compounds were determined by using the modified MTPA Mosher ester method, and by circular dichroism (CD) measurements in combination with quantum chemical CD calculations. The structures of these limonoids hint at a new biosynthetic pathway to tetranortriterpenoids.

Results and Discussion

Isolation of xylogranatins C, D, and F–R (1–13): The dried seeds of *X. granatum* were extracted with ethanol. The extract was concentrated and partitioned between water and petroleum ether. The aqueous layer was further extracted with ethyl acetate and concentrated to give a brown gum, which was subjected to silica-gel chromatography (chloroform/methanol 100:0 to 2:1). The fractions that were eluted with chloroform/methanol (25:1 to 15:1) were combined and purified by repetitive C_{18} HPLC to afford xylogranatins C, D, and F–R (**1**–**13**).

Structural elucidation of xylogranatins F–H (1–3): Xylogranatin F (**1**), an amorphous powder, had a molecular formula of $C_{26}H_{27}NO_6$, which was established by HR-TOFMS (m/z: calcd: 472.1736; found: 472.1724 $[M+Na]^+$). The ^1H and ^{13}C NMR spectroscopy data (Table 1) indicated that the molecule contained a carbon–nitrogen double bond, five carbon–carbon double bonds, two carbonyls, and six ring systems. DEPT experiments revealed that **1** had four tertiary methyls, three methylenes, eight methines (of which five are olefinic), and eleven quaternary carbon atoms. In addition, the NMR spectroscopic data (Table 1) showed the presence of a hydroxyl, $\delta_H = 2.24$–2.28 ppm (brs), and a β-furyl ring ($\delta_H = 6.52$ (brs), 7.48 (brs), 7.56 (brs), $\delta_C = 110.0$ (d), 119.8 (s), 141.4 (d), 143.3 ppm (d)). Three substructures **1a** (from C11 to C18 and from C20 to C23), **1b** (from C3 to C7, C10, C19, C28, and C29) and **1c** (from C1 to C2, C30, and from C8 to C9) (Figure 1a) were determined by analysis of the 2D ^1H-^1H COSY, HSQC, and HMBC spectral data of **1**. Substructure **1a** was elucidated by starting from an α,β-unsaturated δ-lactone ring D, which was characterized by the following NMR spectroscopic data: $\delta_H = 6.57$ (s), 5.22 (s); $\delta_C = 37.7$ (s), 157.2 (s), 111.2 (d), 165.2 (s), 80.9 ppm (d), and was corroborated by the HMBC correlations between H15/C13, H15/C14, H15/C16, H17/C13, and H17/C16 (Figure 1a). The HMBC cross-peaks from H17 to C20, C21, and C22 indicated that the β-furyl ring is connected to C17 of the δ-lactone ring D. A methyl singlet resonance at $\delta_H = 1.15$ ppm (Me18) and the methylene protons of C12, which show HMBC correlations to the γ-C (C13) of ring D along with a proton spin system, $H_2$11–$H_2$12, which was deduced from the ^1H-^1H COSY correlations, permitted us to establish the connections of this proton spin system and Me18 with C13. Taken together, the above data gave substructure **1a**. The second fragment, substructure **1b**, could be assembled by starting from the γ-lactone ring F, which was characterized by the NMR spectroscopic data: $\delta_H = 2.97$ (d, $J = 9.5$ Hz), 2.58 (dd, $J = 17.2$, 2.4 Hz), 2.98 (dt, $J = 17.2$, 9.5 Hz); $\delta_C =$ 45.8 (d), 31.0 (t), 175.2 (s), 84.1 ppm (s), and was confirmed by ^1H-^1H COSY correlations from H5 to $H_2$6 and HMBC cross-peaks from H5 to C6, C7, and C10 (Figure 1a). The methyl singlet resonance at $\delta = 1.83$ ppm (Me19) has HMBC correlations with β-C (C5) and γ-C (C-10) of the γ-lactone, revealing that it is attached to the γ-C (C10). A proton singlet of a methine (H3), which bears a hydroxyl resonance at $\delta_H = 4.48$ ppm and two methyl singlet resonances at $\delta = 1.16$ (Me28) and 0.83 ppm (Me-29), respectively, exhibits HMBC cross-peaks to a quaternary carbon (C4) and the β-C (C5) of the above γ-lactone; this suggests that the quaternary carbon (C4), which bears two methyl groups is situated be-

Table 1. ^{1}H (500 MHz) and ^{13}C NMR (125 MHz) spectroscopic data for xylogranatins F–H (**1**–**3**).[a]

Position	**1** ($CDCl_3$)		**2** ($CDCl_3$)		**3** (CD_3OD)	
	^{1}H δ [ppm]	^{13}C δ [ppm]	^{1}H δ [ppm]	^{13}C δ [ppm]	^{1}H δ [ppm]	^{13}C δ [ppm]
1		156.7 (s)		156.9 (s)		153.2 (s)
2		130.6 (s)		126.8 (s)		132.5 (s)
3	4.48 (s)	75.6 (d)	5.60 (s)	76.7 (d)	4.37 (s)	76.3 (d)
4		36.3 (s)		35.2 (s)		37.3 (s)
5	2.97 (d) 9.5	45.8 (d)	2.93 (d) 9.2	45.5 (d)	2.94 (d) 9.2	47.0 (d)
6α 6β	2.58 (dd) 17.2 2.4 2.98 (dt) 17.2 9.5	31.0 (t)	2.61 (dd) 18.0 1.5 3.05 (dd) 18.0 9.2	30.8 (t)	2.62 (dd) 18.0 2.9 3.13 (m)[b]	31.8 (t)
7		175.2 (s)		174.8 (s)		174.5 (s)
8		124.3 (s)		124.3 (s)		134.7 (s)
9		158.1 (s)		158.7 (s)		158.2 (s)
10		84.1 (s)		83.6 (s)		86.0 (s)
11α, 11β	3.10 (dd); 18.5 5.0, 3.20 (dd) 18.5 4.0	28.0 (t)	3.13 (dd); 18.5 5.0 3.20 (dd), 18.5 4.0	28.1 (t)	2.96 (dd); 19.0 5.0, 3.09 (dd) 19.0 4.0	28.8 (t)
12α 12β	1.87 (dd) 13.0 4.0 1.75 (dt) 13.0 5.0	30.3 (t)	1.87 (dd) 13.0 4.0 1.73 (dt) 13.0 5.0	30.2 (t)	1.96 (dd) 13.0 4.0 1.73 (dt) 13.0 5.0	31.5 (t)
13		37.7 (s)		37.6 (s)		37.6 (s)
14		157.2 (s)		156.5 (s)	3.15[b] m	41.8 d
15α, 15β	6.57 (s)	111.2 d	6.59 (s)	111.7 (d)	3.02 (dd) 16.0 6.0 2.88 (dd) 16.0 11.5	36.8 (t)
16		165.2 (s)		164.8 (s)		178.5 (s)
17	5.22 (s)	80.9 (d)	5.21 (s)	80.9 (d)	5.44 (s)	81.0 (d)
18	1.15 (s)	15.8 (q)	1.14 (s)	15.8 (q)	1.03 (s)	22.5 (q)
19	1.83 (s)	28.5 (q)	1.80 (s)	28.6 (q)	1.79 (s)	28.6 (q)
20		119.8 (s)		119.9 (s)		122.4 (s)
21	7.56 (brs)	141.4 (d)	7.55 br(s)	141.4 (d)	7.66 br(s)	142.6 (d)
22	6.52 (brs)	110.0 (d)	6.51 (brs)	110.1 (d)	6.61 (brs)	111.0 (d)
23	7.48 (brs)	143.3 d	7.48 (brs)	143.3 (d)	7.59 (brs)	144.7 (d)
28	1.16 (s)	23.5 (q)	1.13 (s)	23.9 (q)	1.15 (s)	24.1 (q)
29	0.83 (s)	21.4 (q)	0.78 (s)	20.3 (q)	0.72 (s)	21.4 (q)
30	8.05 (s)	133.9 (d)	8.14 (s)	135.7 (d)	7.69 (s)	139.6 (d)
3-OH	2.24–2.28 (brs)					
3-OAc			2.06 (s)	20.9 (q) 170.1 (s)		

[a] Multiplicities are indicated in parentheses. [b] Overlapped signals without designating multiplicity.

tween C3 and C5. This connection was corroborated by the HMBC correlation from H5 to C4. From these data, the second substructure was unambiguously deduced as **1b**. The final fragment, **1c**, was assembled as a tetrasubstituted pyridine ring on the basis of the NMR spectroscopic data (δ_H = 8.05 (s), δ_C = 124.3 (s), 130.6 (s), 133.9 (d), 156.7 (s), 158.1 ppm (s); Table 1) and the HMBC correlations from H30 to C1, C2, and C9. This identification was consistent with the result that **1** was a nitrogenous compound, which was deduced from its molecular formula. Obviously, HMBC correlations were crucial in assembling the gross structure of xylogranatin F (**1**). Briefly, cross-peaks Me19/C1, H3/C1, H3/C2, and H3/C30, connected substructures **1b** and **1c** to each other through the carbon–carbon bonds of C1−C10 and C2−C3, whilst HMBC correlations H11/C8, H11/C9, H30/C11, H30/C14, H15/C8 linked fragments **1c** and **1a** together by the carbon–carbon bonds of C8−C14 and C9−C11 (Figure 1a). From all these observations, the constitution of **1** was attributed to xylogranatin F as shown in Figure 1.The relative configuration of **1** was established on the basis of the NOESY spectrum. The significant NOE interactions that were observed in **1** (Figure 1b) H3/H5, H3/H6β, H3/H30, H3/Me19, H3/Me28, H5/H6β, and H5/Me19 indicated their mutual *cis* relationship and the *cis*-fused orientation of rings A/F. The above NOE observations also helped to establish a β configuration for H3. Similarly, the interactions H17/H22, H17/H12β, H17/H15, Me18/H21, Me18/H15, and H30/H15, suggested that the configuration of Me18 is α and H17 is β and the furyl ring α configured. Moreover, the NOE interactions between H3 and H30, and between H15 and H30, established the (s)-*cis*-conformation that is displayed in the carbon series C3–C2–C30–C8–C14–C15. Based on the above results, the relative stereostructure of **1** was elucidated as shown in Figure 1b.

Acetylation of **1** with acetic anhydride in pyridine afforded 3-*O*-acetyl xylogranatin F (Scheme 2), which was also isolated from the seeds of *X. granatum* as a natural product, and was named xylogranatin G (**2**). This corroborated the observation that the free hydroxyl group of **1** was located at C3. The relative configuration of C3 in **2** was established to be the same as in **1** on the basis of the NOE interactions H3/H5, H3/H30, H3/Me19, and H3/Me28 (see Figure S1 in

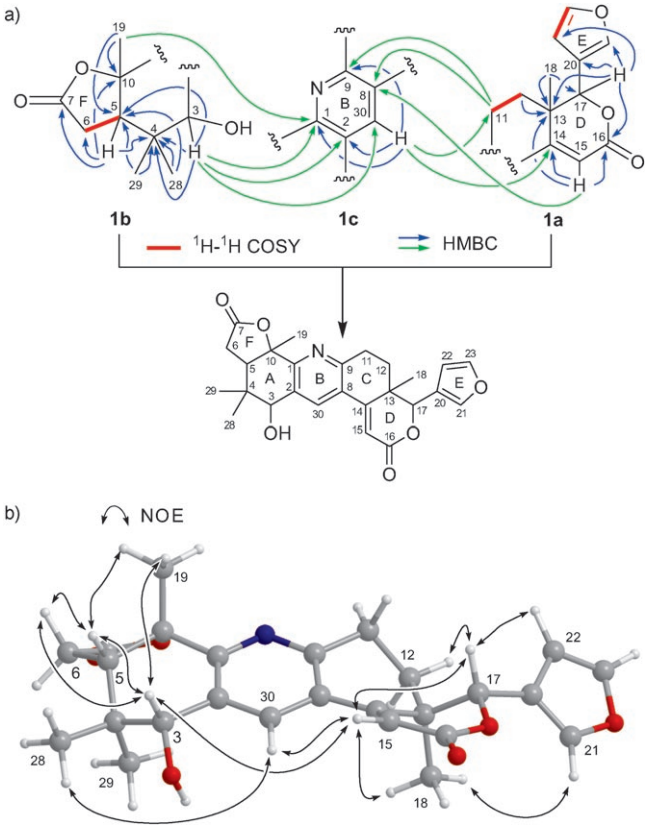

Figure 1. a) Partial structures, and the ^{1}H-^{1}H COSY or HMBC correlations that were used to establish the gross structure of xylogranatin F (**1**) (blue arrows indicate interactions within the fragments, green ones between them). b) Significant NOE correlations for xylogranatin F (**1**).

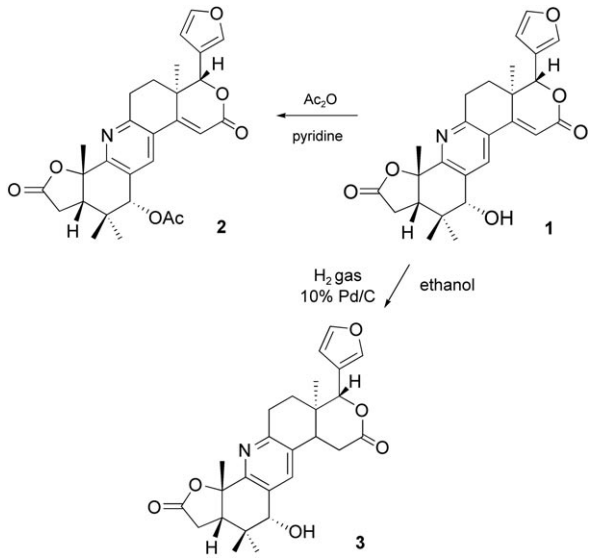

Scheme 2. Chemical correlations for xylogranatins F–H (**1**–**3**).

the Supporting Information). Based on the above results, the relative (and thus) absolute configuration of **1** and **2** was determined to be the same.

Xylogranatin H (**3**), was isolated as an amorphous powder, and was found to have a molecular formula of $C_{26}H_{29}NO_6$ (i.e., larger than that of **1** by two hydrogen atoms); this was established by HR-TOFMS spectrometry (m/z: calcd: 474.1893; found: 474.1884 $[M+Na]^+$). The ^{1}H and ^{13}C NMR spectroscopic data (Table 1) of **3** were similar to those of **1**. This suggests that **3** might have the same basic molecular framework as **1**. However, an olefinic proton ($\delta_H = 6.57$ (s), H15 in **1**) and two olefinic carbons ($\delta_C = 157.2$ (s), 111.2 (d), C14 and C15 in **1**) that were derived from the double bond C14=C15 in **1** were absent in **3**, but an aliphatic proton spin system, H14–H$_2$15 ($\delta_H = 3.15$ (m), 2.88 (dd, J = 16.0, 11.5 Hz), 3.02 ppm (dd, J = 16.0, 6.0 Hz); $\delta_C = 41.8$ (d), 36.8 ppm (t)) appeared in **3**; this was deduced from ^{1}H-^{1}H COSY correlations, and indicated that the C14=C15 double bond of **1** was hydrogenated in xylogranatin H (**3**). HMBC correlations from H14 and H$_2$15 to C8, C13, C15, and C16 corroborated that the C14=C15 double bond of the compound was a hydrogenated analogue of **1**. The NOE interaction that was observed in **3** from Me18 to H14 indicated the α configuration of H14, and the interactions between H3/H5, H3/H6, H3/H30, H3/Me19, and H3/Me28 (see Figure S2 in the Supporting Information) established 3β-H and the inverse 3α-OH group. The chemical transformation from **1** to **3** by catalytic hydrogenation (10% Pd/C in ethanol) (Scheme 2) further confirmed the structure that is shown in Scheme 1.

Absolute stereostructures of xylogranatins F–H (1–3): The above NOE correlation studies on compounds **1**–**3** and chemical transformations from compound **1** to **2** and **3** confirmed that the absolute configurations of compounds **1**–**3** were identical (Scheme 2). As shown in Scheme 1, the central molecular portion of compounds **1**–**3** is a pyridine ring. It divides each of them into two relatively isolated, NOE-independent substructures. Within one such substructure, the stereochemical assignment of one single stereogenic element will unambiguously establish the absolute configuration of the entire substructure. Each of the substructures **1b** of **1** and fragment **3b** of **3** (Figure 2) has a secondary alcohol at C3. Consequently, the absolute stereostructure of this chiral center, which was the same in compounds **1**–**3**, could be determined by using the modified Mosher MTPA [α-methoxy-α-(trifluoromethyl)phenylacetyl] ester method.[21] On the other hand, substructure **1a** of compound **1** has two main

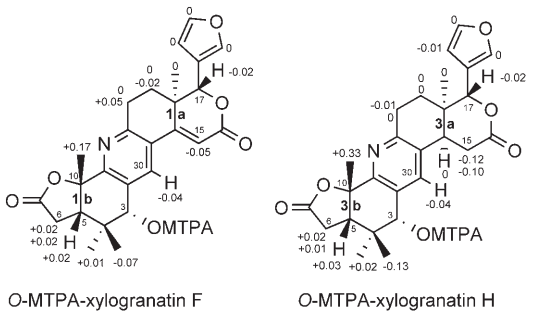

O-MTPA-xylogranatin F *O*-MTPA-xylogranatin H

Figure 2. Δδ values (Δδ [ppm] = [$\delta_S - \delta_R$]) obtained for the (3*S*) and (3*R*)-MTPA esters of xylogranatin F (**1s**, **1r**) and H (**3s**, **3r**).

chiral chromophores, one is a furan ring and the other one is the α,β-unsaturated δ-lactone that is conjugated with a pyridine ring. Both are connected through the chiral center of C17 in substructure **1a** (Figure 2). Therefore, it should be possible to determine the absolute configuration of C17 in portion **1a** by circular dichroism (CD) analysis.

The modified Mosher method was employed to determine the absolute configuration of C3 in **1** and **3** (Figure 2). Unfortunately, in xylogranatin F (**1**), the $\Delta\delta$ values of a methyl and one proton, that is, Me28 ($\Delta\delta = -0.07$ ppm) in substructure **1b** and H11β ($\Delta\delta = +0.05$ ppm) in **1a**, disobeyed the Mosher rule. Other protons, however, did obey the rule. The $\Delta\delta$ values of all protons in substructure **1b**, except for those of Me28, were positive, while those in **1a**, except for that of H11β, were negative. This regular arrangement indicated that the configuration of C3 in **1** might be *R*. In xylogranatin H (**3**), the $\Delta\delta$ values of all protons in substructure **3b**, except for that of Me28 ($\Delta\delta = -0.13$ ppm) were positive, while those in **3a** were all negative. This observation suggested the 3*R* configuration in **3**. The result is consistent with that of the above-described chemical transformation from **1** to **3** and the NOE correlation studies on compounds **1** and **3**, which had shown that the configuration at C3 in the two compounds was the same. The irregular $\Delta\delta$ values of Me28 in **1** and **3** might be due to steric interactions of the MTPA group with Me28 and other groups of these compounds.[21]

After having established the absolute configuration of **1b** by the Mosher method, and the relative configuration within **1a** by NOE data, two possible isomers remained: the diastereomers (3*R*,5*S*,10*S*,13*R*,17*R*)-**1** and (3*R*,5*S*,10*S*,13*S*,17*S*)-**1**. For the determination of the absolute configuration of **1a** (and thus of the entire molecule **1**), CD investigations were performed in combination with quantum chemical CD calculations. These calculations at the B3LYP/6–31G(d)[22,23] level provided six minima for (3*R*,5*S*,10*S*,13*R*,17*R*)-**1** and four for (3*R*,5*S*,10*S*,13*S*,17*S*)-**1** with a relevant contribution to the overall CD spectra (Tables S1 and Table S2).[24] In both cases, the single CD curves of these structures were added up by following the Boltzmann statistic, and then were UV corrected (red shift of $\lambda = 10$ nm for the calculated CD spectra).[25] The comparison of the theoretical curves with the experimental ones (Figure 3) revealed that nearly all the calculated Cotton effects of (3*R*,5*S*,10*S*,13*S*,17*S*)-**1** are opposite to the ones that were experimentally obtained, whereas the curve that was simulated for (3*R*,5*S*,10*S*,13*R*,17*R*)-**1** reproduces the experimental spectrum in the range from $\lambda = 240$–400 nm very well, expect for the peak at $\lambda = 230$ nm. By model calculations in which **1** was divided into two chromophores (see Figure S3 in the Supporting Information), it could be shown that this unexpected peak originates from the moiety **1b**, of which the absolute configuration is known by applying the Mosher method. Therefore, this peak is most probably an artifact of the applied theoretical method, and could be neglected. From the model calculations, we also know that the northeastern chromphore with the stereocenters at C13 and C17

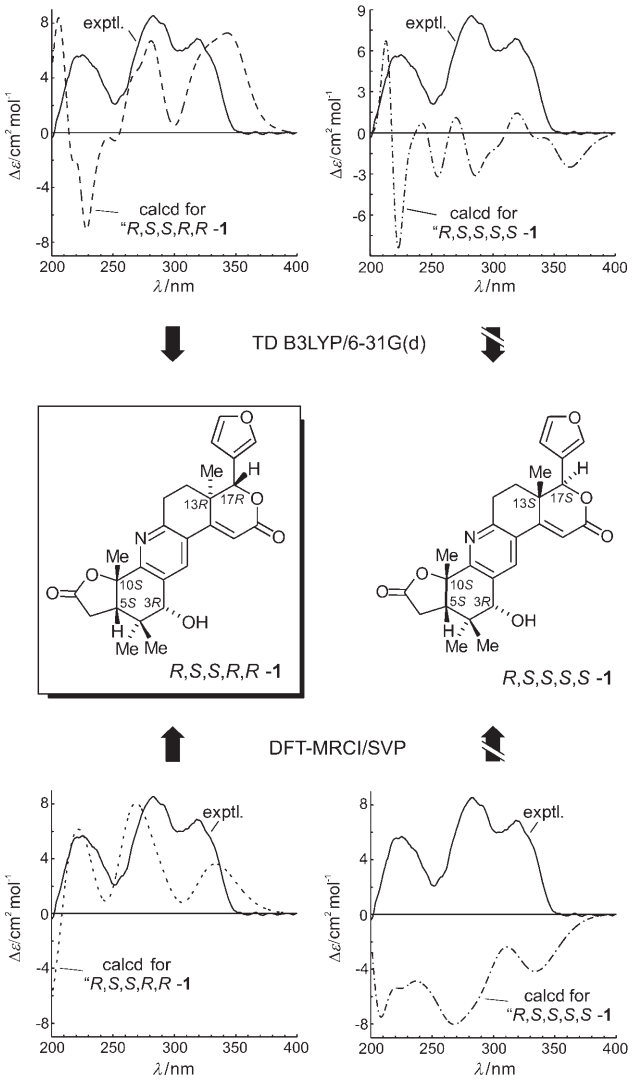

Figure 3. Comparison of the calculated CD spectra (top: TDB3LYP/6–31G(d) results; bottom: DFT/MRCI/SVP results) of the remaining possible diastereomers of **1**, (3*R*,5*S*,10*S*,13*R*,17*R*)-**1** and (3*R*,5*S*,10*S*,13*S*,17*S*)-**1**, with the measured CD curve: Only the spectrum calculated for (3*R*,5*S*,10*S*,13*R*,17*R*)-**1** fits with the experimental one.

dominate the chiroptical properties of the molecule, which is the reason why the CD spectra of the two possible diastereomers are nearly mirror-image-like. Nonetheless, with DFT/MRCI/SVP[26,27] we also used a higher level of theory to calculate the CD spectra of the above-found conformers. As expected, the results of these calculations clearly proved our first assignment of the absolute configuration from the time-dependent DFT (TDDFT) results, because only the curve that was calculated for (3*R*,5*S*,10*S*,13*R*,17*R*)-**1** fits very well the experimental one. Furthermore, no unexpected peak was observed, which corroborated our assumption that the non-fitting peak in the TDDFT calculations is indeed an artifact of the method that was used. In combination with the experimental results, the calculations thus unambiguously showed that C13 and C17 of xylogranatine F (**1**) are both *R*-configured.

Structural elucidation of xylogranatins I–R (4–13): The TOFMS of xylogranatin I (**4**) showed the molecular-ion peak at *m*/*z*: 500. Its molecular formula was established to be $C_{27}H_{32}O_9$ by HR-TOFMS (*m*/*z*: calcd: 500.2046; found: 500.2052 $[M]^+$). This together with the ^1H and ^{13}C NMR spectroscopic data (see the Experimental Section and Table 2) indicated the presence of five carbon–carbon double bonds and three carbonyls, as well as four iso- or heterocyclic rings. DEPT experiments revealed that **4** had five methyls, three methylenes, nine methines (five of them olefinic), and ten quaternary carbon atoms. In addition, the NMR spectroscopic data (see the Experimental Section and Table 2) showed the presence of a β-furyl ring ($\delta_H = 6.53$ (brs), 7.53 (brs), 7.67 (brs); $\delta_C = 111.1$ (d), 122.0 (s), 143.6 (d), 144.7 ppm (d)).Three substructures **4a** (from C9, C11 to C18, and from C20 to C23), **4b** (from C3 to C7, C10, C19, C28, and C29), and **4c** (from C1 to C2, C8, and C30) were determined by analysis of the 2D ^1H-^1H COSY, HSQC, and HMBC spectra of **4** (Figure 4a). Substructure **4a** was elucidated by starting from an α,β-unsaturated δ-lactone ring D, which is characterized by the following NMR spectroscopic data: $\delta_H = 6.39$ (s), 5.52 (s); $\delta_C = 41.9$ (s), 153.7 (s), 113.1 (d), 167.1 (s), 79.5 ppm (d). This was corroborated by the HMBC correlations: H15/C13, H15/C14, H15/C16, H17/C13, and H17/C16 (Figure 4a). The HMBC cross-peaks from H17 to C20, C21, and C22 indicated that the β-furyl ring is connected to C17 of the δ-lactone ring D. A methyl singlet resonance at $\delta_H = 1.27$ ppm (Me18) and the protons of C12, which show HMBC correlations to the γ-C (C13) of ring D, established the connections between $CH_2$12 and Me18 with C13. HMBC cross-peaks from the protons of the spin system, $H_2$11–$H_2$12 to a carboxyl carbon atom, which was deduced from the ^1H-^1H COSY correlations, linked this proton spin system with a terminal carboxyl. These results established the substructure **4a**.

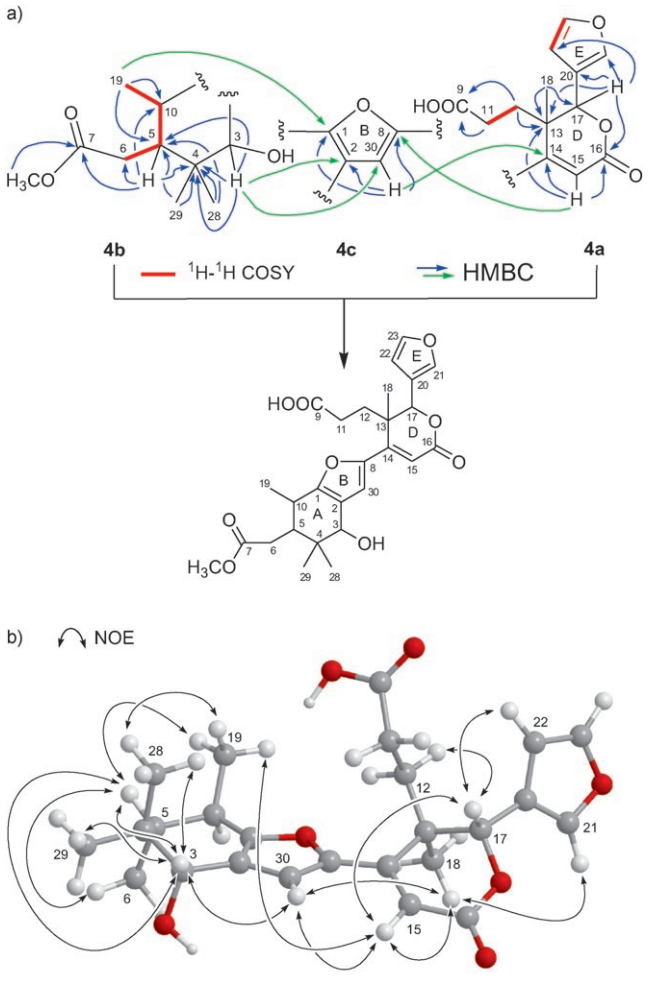

Figure 4. (a) Partial structures, ^1H-^1H COSY and HMBC correlations that are indicative of the gross structure of xylogranatin I (**4**) (blue arrows indicate interactions within the fragments, green ones between them). (b) Significant NOE correlations for xylogranatin I (**4**); to simplify the structure, the CO_2Me group at C6 is omitted).

A second fragment could be assembled as **4b** by starting from the proton spin system H6–H5–H10–H19, which was deduced from ^1H-^1H COSY correlations. HMBC cross-peaks from H6 to the ester carbon atom of a methoxycarbonyl group ($\delta_H = 3.70$ ppm (s); $\delta_C = 52.3$ (q), 176.1 ppm (s)) connected C6 with this terminal group. A proton singlet of a methine (C3), which bears a hydroxyl resonance at $\delta_H =$ 4.05 ppm and two methyl singlet resonances at $\delta_H = 1.05$ (Me29) and 0.76 ppm (Me28), and exhibits HMBC cross-peaks to a quaternary carbon atom (C4) and C5 of the above proton spin system, suggested that the quaternary carbon atom (C4) that bears two methyl groups was situated between C3 and C5. This connection was corroborated by the HMBC correlation from H5 to C4; this gives substructure **4b**.

The last fragment, **4c**, was assembled as a trisubstituted furan ring on the basis of the NMR spectroscopic data ($\delta_H =$ 7.08 ppm (s); $\delta_C = 159.8$ (s), 123.0 (s), 116.7 (d), 149.5 ppm (s)) (Table 2) and HMBC correlations from H30 to C1, C2, and C8. Moreover, the HMBC cross-peaks Me19/C1, H3/C2, H3/C30, connected substructures **4b** and **4c** through the carbon–carbon bonds of C1–C10 and C2–C3, whilst HMBC correlations H30/C14, H15/C8, linked fragments **4a** and **4c** together through the interaction of C8–C14. From all these observations, the planar structure of **4** was identified as shown in Figure 4.

The relative stereostructure of **4** was established on the basis of the NOESY spectrum. The significant NOE interactions observed in **4** (Figure 4b) H3/H5, H3/H30, H3/Me29, H5/H6b, H5/Me19, indicated they are *cis* to each other. The above NOE observations also helped to establish 3β-H and the inverse 3α-hydroxyl group. Similarly, the interactions between H17/H22, H17/H12b, H17/H15, Me18/H30, Me18/H21, Me18/H15, H30/H15, suggested that Me18 is α, H17 is β, and the β-furyl ring at C17 is therefore α. The observed NOE correlations between Me18 and H17, although seemingly not in agreement with the bisaxial array in the global minimum that was found by the DFT calculations, can, however, be explained by one of the other conformers, in which these two substituents adopt a bisequatorial orientation; this leads to a close proximity of these two spin systems

Table 2. ^{13}C NMR (125 MHz) data for xylogranatins I–R (**4**–**12** in [D_4]methanol and **13** in $CDCl_3$).[a]

Position	4	5	6	7	8	9	10	11	12	13
1	159.8 (s)	160.4 (s)	160.3 (s)	160.2 (s)	161.1 (s)	161.0 (s)	161.1 (s)	161.0 (s)	158.9 (s)	200.5 (s)
2	123.0 (s)	120.9 (s)	120.8 (s)	121.5 (s)	119.9 (s)	120.1 (s)	120.1 (s)	120.0 (s)	125.2 (s)	129.3 (s)
3	72.9 (d)	82.3 (d)	82.3 (d)	80.7 (d)	75.0 (d)	74.8 (d)	75.0 (d)	74.8 (d)	81.6 (d)	159.2 (d)
4	40.2 (s)	40.2 (s)	40.2 (s)	40.2 (s)	39.1 (s)	39.2 (s)	39.5 (s)	39.3 (s)	43.8 (s)	36.9 (s)
5	42.7 (d)	43.2 (d)	43.2 (d)	43.4 (d)	43.6 (d)	43.7 (d)	43.7 (d)	43.7 (d)	54.7 (d)	45.6 (d)
6	34.5 (t)	34.5 (t)	34.5 (t)	34.6 (t)	34.3 (t)	34.2 (t)	34.1 (t)	34.2 (t)	84.3 (d)	34.7 (t)
7	176.1 (s)	176.1 (s)	176.1 (s)	176.2 (s)	176.0 (s)	175.9 (s)	176.0 (s)	175.9 (s)	174.3 (s)	173.6 (s)
8	149.5 (s)	149.3 (s)	149.2 (s)	149.3 (s)	149.7 (s)	149.7 (s)	149.7 (s)	149.8 (s)	150.6 (s)	197.8 (s)
9	176.4 (s)	174.9 (s)	176.5 (s)	176.8 (s)	174.8 (s)	–[b]	–[b]	174.9	175.9 (s)	175.5 (s)
10	34.5 (d)	34.8 (d)	34.8 (d)	34.8 (d)	34.5 (d)	34.4 (d)	34.4 (d)	34.5 (d)	40.8 (d)	43.1 (d)
11	30.1 (t)	30.1 (t)	30.2 (t)	30.5 (t)	30.1 (t)	30.8	–[b]	–[b]	30.5 (t)	29.8 (t)
12	33.1 (t)	33.1 (t)	33.1 (t)	33.3 (t)	33.2 (t)	–[b]	–[b]	–[b]	33.1 (t)	29.8 (t)
13	41.9 (s)	42.0 (s)	42.0 (s)	42.0 (s)	41.9 (s)	42.4 (s)	42.0 (s)	42.0 (s)	42.0 (s)	41.5 (s)
14	153.7 (s)	153.7 (s)	153.9 (s)	154.0 (s)	153.4 (s)	153.8 (s)	153.7 (s)	153.9 (s)	153.8 (s)	158.8 (s)
15	113.1 (d)	113.4 (d)	113.3 (d)	113.2 (d)	114.0 (d)	113.7 (d)	113.7 (d)	113.7 (d)	113.5 (d)	124.6 (d)
16	167.1 (s)	167.1 (s)	167.1 (s)	167.2 (s)	166.9 (s)	167.0 (s)	167.1 (s)	167.1 (s)	167.1 (s)	163.4 (s)
17	79.5 (d)	79.6 (d)	79.5 (d)	79.6 (d)	79.5 (d)	79.7 (d)	79.6 (d)	79.7 (d)	79.5 (d)	78.6 (d)
18	21.5 (q)	21.4 (q)	21.4 (q)	21.5 (q)	21.4 (q)	21.6 (q)	21.5 (q)	21.5 (q)	21.4 (q)	20.4 (q)
19	16.7 (q)	16.9 (q)	16.9 (q)	16.9 (q)	16.6 (q)	16.8 (q)	16.8 (q)	16.8 (q)	17.5 (q)	11.8 (q)
20	122.0 (s)	122.0 (s)	122.0 (s)	122.1 (s)	122.0 (s)	122.1 (s)	122.0 (s)	122.1 (s)	121.9 (s)	119.4 (s)
21	143.6 (d)	143.7 (d)	143.6 (d)	143.6 (d)	143.7 (d)	143.7 (d)	143.7 (d)	143.7 (d)	143.6 (d)	141.6 (d)
22	111.1 (d)	111.0 (d)	111.1 (d)	111.1 (d)	111.0 (d)	111.1 (d)	111.1 (d)	111.1 (d)	111.1 (d)	109.8 (d)
23	144.7 (d)	144.8 (d)	144.7 (d)	144.7 (d)	144.8 (d)	144.7 (d)	144.7 (d)	144.7 (d)	144.7 (d)	143.5 (d)
28	20.0 (q)	20.0 (q)	20.0 (q)	20.1 (q)	19.7 (q)	19.7 (q)	19.6 (q)	19.7 (q)	22.4 (q)	20.2 (q)
29	25.0 (q)	25.1 (q)	25.1 (q)	25.2 (q)	24.5 (q)	24.8 (q)	24.7 (q)	24.6 (q)	26.3 (q)	28.2 (q)
30	116.7 (d)	117.2 (d)	117.2 (d)	117.0 (d)	116.8 (d)	116.8 (d)	116.9 (d)	116.8 (d)	115.2 (d)	41.4 (t)
7-OMe	52.3 (q)	52.4 (q)	52.3 (q)	52.3 (q)	52.4 (q)	52.4 (q)	52.4 (q)	52.4 (q)	52.8 (q)	52.0 (q)
9-OMe		52.3 (q)			52.3 (q)					
3-R^2										
1′		57.5 (q)	57.5 (q)	66.2 (t)	172.7 (s)	177.8 (s)	169.1 (s)	178.3 (s)		
2′				15.8 (q)	21.0 (q)	42.8 (d)	129.8 (s)	35.4 (d)		
3′						27.9 (t)	139.2 (d)	19.4 (q)		
4′						11.9 (q)	12.2 (q)	19.2 (q)		
5′						17.1 (q)	14.5 (q)			

[a] Multiplicites are shown in parentheses and δ values are in ppm. [b] Not detected.

(Figure 5). The same NOE correlations with similar intensities had previously been observed in a closely related structure, xyloccensin O, the *trans* configuration of Me18 and H17 of which was further supported by X-ray diffraction.[28]

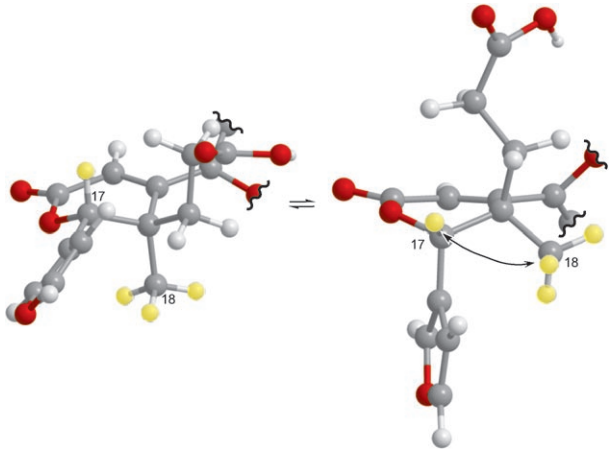

Figure 5. Two main conformations of ring D in xylogranatins I–Q (**4**–**12**) with H17 and Me18 in bisaxial (left) and bisequatorial (right) orientation; this explains the observed NOE correlations between H17 and Me18, although they are *trans* configured. For reasons of clarity, only rings D and E are shown (cut at C30 and the furan oxygen).

The important NOE interaction that was observed in **4** was Me19/H15; this suggested that the configuration of Me19 is β, which was simultaneously the key NOE juncture between the substructures **4a** and **4b**. Based on the above results, the relative structure of **4** was elucidated as shown in Figure 4b.

The absolute configuration of **4** was established by the application of the same two-step method that was used for xylogranatins F–H above. Thus, the absolute configuration of the secondary alcohol that bears center C3 in **4b** (Figure 4a) was determined by using the modified Mosher MTPA ester method. The chiral center at C17 in substructure **4a** (Figure 4a) was again established by comparing the experimental CD spectrum of **4** with the spectra that was predicted by quantum chemical calculations for each of the two remaining possible diastereomers and their enantiomers.

Owing to the low reactivity of the secondary hydroxyl group at C3 of **4** towards MTPACl, it was difficult to obtain the (3*S*)- and (3*R*)-MTPA esters of **4**. Thus, treatment of **4** with (*R*)- and (*S*)-MTPACl in dichloromethane solvent, with a mixture of diethylamine, triethylamine, and (dimethylamino)pyridine (DMAP) as a catalyst, did not yield the desired esterified products, but the 9-diethylamide **4′** instead (Figure 6). To our surprise, when this derivative was treated

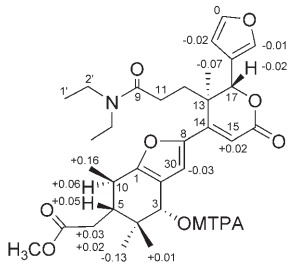

Figure 6. $\Delta\delta$ values [$\Delta\delta$ (ppm) $=(\delta_S-\delta_R)$] that were obtained for the (3*S*) and (3*R*)-MTPA esters (**4′s**, **4′r**) of the 9-diethylamide derivative of xylogranatin I.

with (*R*)- and (*S*)-MTPACl in pyridine, with DMAP at room temperature, its 3-(*S*) and 3-(*R*)-MTPA esters (**4′s**, **4′r**) were formed in high yields; this permitted us to assign the absolute configuration of C3 in **4**.

As shown in Figure 6, the $\Delta\delta$ values of H5, H6, H10, H19, H28 were positive, while those of H17, H18, H21, H22, and H30 were negative. This regular arrangement provided evidence for the 3*R* configuration in **4′**. Because the absolute stereostructure of **4** must be the same as that of its derivative **4′**, the absolute configuration of C3 in **4** was then assigned as *R* too. Based on this 3*R* configuration, the chirality of C10 in **4** was also identified as *R* through NOE investigations, which led to 19βMe. This result was consistent with the NOE interaction observed earlier in **4** from Me19 to H15.

Me29 and H15 in **4′**, by contrast, disobeyed Mosher's rule. The steric interactions with the MTPA group from Me29 and other groups inside **4′** with that in xylogranatin F and H could explain why Me29 disobeys this rule,[21] and the different rotation effects on the C8–C14 bond that is induced by the (3*S*) and (3*R*)-MTPA esters might explain why H15 disobeys Mosher's rule. This might be a consequence of a change of the dihedral angle between the central furan ring and the α,β-unsaturated δ-lactone according to the different substituents at 3-OH. In **4′s** and **4′r**, this dihedral angle was different. Thus the shielding and deshielding effects from the benzene ring of MTPA esters to H15 was not as regular as those of the other protons in **4′**.

Because the Mosher method did not lead to an unambiguous result in this case, the experimental CD spectrum of **4** had to be compared with the spectra that were computed for all four possible diastereomers of **4**, which resulted from the combination of all enantiomeric forms of the substructures with the relative configurations that were established by the NOE measurements above. For this purpose, TDDFT calculations of the twelve energetically lowest conformers of **4A** (3*R*,5*R*,10*R*,13*R*,17*R*-**4**) and of the twelve energetically lowest ones of **4B** (3*R*,5*R*,10*R*,13*S*,17*S*-**4**) were carried out (see also Tables S3 and S4 in the Supporting Information). The CD spectra of the respective enantiomers, *ent*-**4A** (3*S*,5*S*,10*S*,13*S*,17*S*-**4**) and *ent*-**4B** (3*S*,5*S*,10*S*,13*R*,17*R*-**4**), were obtained by reflecting at the zero line of the spectra that was simulated for **4A** and **4B**, respectively. After Boltzmann weighting and UV shifting (red shift of $\lambda=8$ nm for the calculated CD spectra) the comparison of the calculated spectra with the experimental one showed only one match. The simulated CD spectrum of **4B** has only one Cotton effect at $\lambda=350$ nm that fits to the experimental curve, one at $\lambda=230$ nm that is slightly shifted in comparison to the experiment, and two effects at $\lambda=240$ and 260 nm which are opposite to the experiment (Figure 7). Because *ent*-**4B** is the mirrored spectrum of **4B**,

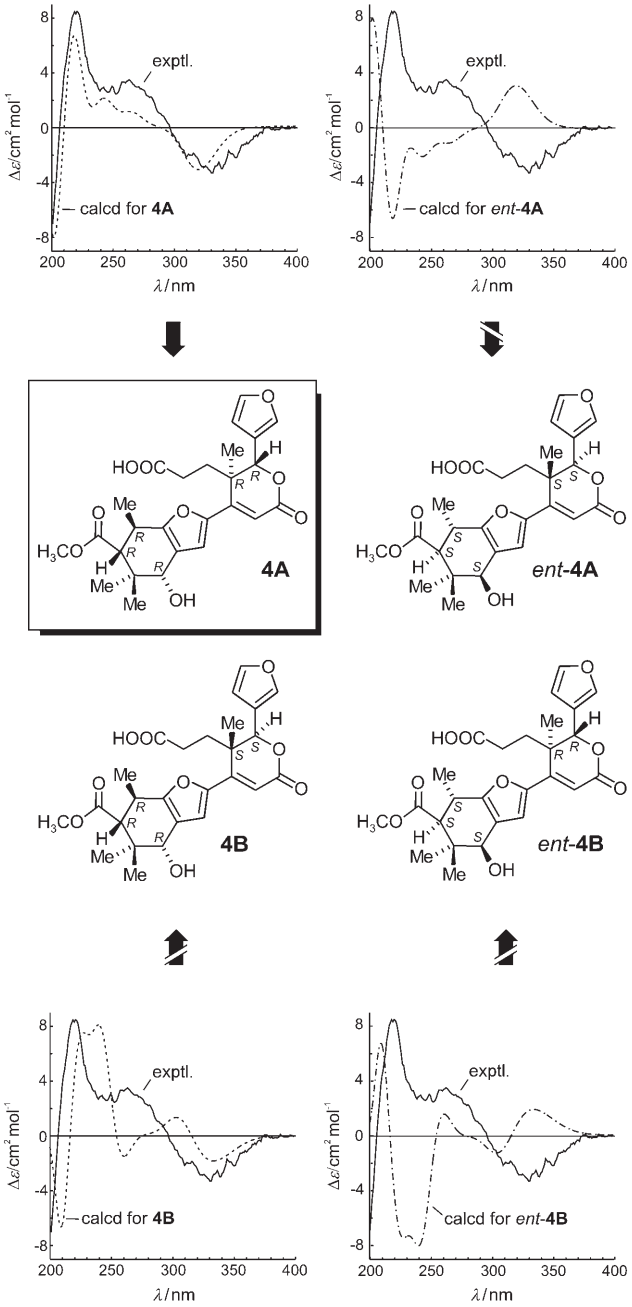

Figure 7. Attribution of the absolute configuration of xylogranatin I (**4**) by comparison of the CD spectra that were calculated for **4A** (3*R*,5*R*,10*R*,13*R*,17*R*-**4**) and **4B** (3*R*,5*R*,10*R*,13*S*,17*S*-**4**) and their enantiomers *ent*-**4A** (3*S*,5*S*,10*S*,13*S*,17*S*-**4**) and *ent*-**4B** (3*S*,5*S*,10*S*,13*R*,17*R*-**4**) with the experimental curve: The spectrum that was calculated for *ent*-**4A** is completely opposite, while the one that was simulated for **4A** fits with the experimental one.

the peaks at $\lambda = 230$ and 350 nm are opposite and the peak at 260 nm coincides with the experiment. Consequently, neither **4B** nor *ent*-**4B** corresponds to the absolute stereostructure of natural xylogranatin I (**4**).

As Figure 7 shows, the computed CD spectrum of **4A**, however, does fit well to the experimental one, whereas the spectrum of *ent*-**4A** is completely opposite compared with the experiment. Therefore, xylogranatine I (**4**) has the same absolute all-*R* configuration as displayed in structure **4A**. Despite the fact that some protons in **4** disobeyed Mosher's rule (as mentioned above), the assignment of the absolute configuration of the southwestern moiety of **4** was correct and furthermore the calculations clearly showed the *R* configuration of C13 and C17.

The molecular formula of xylogranatin J (**5**) was determined to be $C_{29}H_{36}O_9$ by HR-TOFMS (*m*/*z*: calcd: 551.2257; found: 551.2237 $[M+Na]^+$). It was larger than that of xylogranatin I (**4**) by a C_2H_4 unit. The NMR spectroscopic data of **5** were similar to those of **4**, except for the presence of two more methoxy groups ($\delta_H = 3.63$ (s), $\delta_C = 52.3$ (q); $\delta_H = 3.38$ (s), $\delta_C = 57.5$ ppm (q)). HMBC correlations from the protons ($\delta_H = 3.63$ ppm (s)) of one methoxy group to C9 of **5** and H3 ($\delta = 3.66$ ppm (s)) of **5** to the carbon atom of another methoxyl ($\delta_C = 57.5$ (q)) revealed that the above two methoxy groups were substituted at C9 and C3 of **5**. Treatment of **4** with 30% hydrochloric acid in methanol, followed by C_{18} HPLC purification, afforded the major product **5** (yield: >90%) (Scheme 3) and the minor one **5′** (yield: <6%) (see Figure S4 in the Supporting Information). By careful NOE studies, it was found that the configuration of C3 in **5** was the same as in **4**, but that in **5′** was opposite (see Figures S5 and S6 in the Supporting Information). Thus, xylogranatin J (**5**) was concluded to be the 3-*O*-methyl-9-methylester analogue of xylogranatin I (**4**).

Xylogranatin K (**6**) had the molecular formula $C_{28}H_{34}O_9$ as revealed by the HR-TOFMS spectrum (*m*/*z*: calcd: 537.2101; found 537.2112 $[M+Na]^+$). The NMR spectroscopic data of **6** were similar to those of **4**, except for the presence of one additional *O*-methyl group ($\delta_H = 3.35$ ppm (s); $\delta_C = 57.5$ ppm (q)). The HMBC correlation from H3 ($\delta = 3.63$ ppm (s)) of **6** to the carbon atom of this methoxy group indicated that it was attached to C3. Treatment of **6** with (trimethylsilyl)diazomethane ($TMSCHN_2$) afforded xylogranatin J (**5**) (Scheme 2). Thus, xylogranatin K (**6**) was assigned as the 3-*O*-methyl analogue of xylogranatin I (**4**), that is, the free carboxylic acid of the methyl ether of xylogranatin J (**5**).

The HR-TOFMS spectrum (*m*/*z*: calcd: 551.2257; found: 551.2268 $[M+Na]^+$) of xylogranatin L (**7**) showed that this compound had the same molecular formula as **5**. The NMR spectroscopic data of **7** were similar to those of **4**, except for the presence of an ethoxy group ($\delta_H = 1.20$ (t, $J = 7.0$ Hz), 3.52 (m), 3.67 (m); $\delta_C = 15.8$ (q), 66.2 ppm (t)]. The HMBC correlation from H3 ($\delta_H = 3.76$ ppm (s)) of **7** to the methylene carbon atom of this ethoxy group suggested that it was attached to C3. Treatment of **4** with bromoethane and sodium hydride in dichloromethane afforded **7** (Scheme 3). The configuration at C3 in **7** was determined to be the same as in **4** by NOE interactions that were observed in **7** from H3 to H5. Based on the above results, xylogranatin L (**7**) was elucidated as the 3-*O*-ethyl analogue of xylogranatin I (**4**).

The molecular formula of xylogranatin M (**8**) was established as $C_{30}H_{36}O_{10}$ by HR-TOFMS (*m*/*z*: calcd: 579.2206; found: 579.2214 $[M+Na]^+$). The NMR spectroscopic data of **8** were similar to those of **5**, except for the absence of a 3-methoxy group ($\delta_H = 3.38$ ppm (s); $\delta_C = 57.5$ ppm (q) in **5**) and presence of one more acetoxy group ($\delta_H = 2.07$ ppm

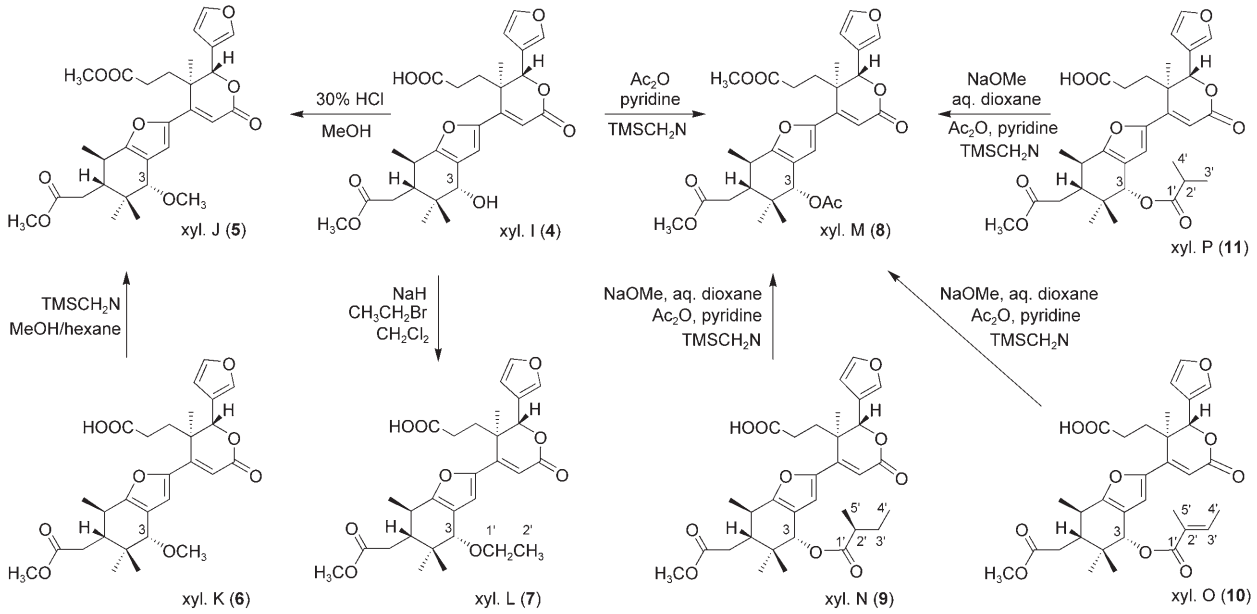

Scheme 3. Chemical correlations for xylogranatins I–P (**4**–**11**) (xyl. = xylogranatin).

(s); $\delta_C = 21.0$ (q), 172.7 ppm (s) in **8**). This result was further corroborated by the HMBC correlation from H3 ($\delta =$ 5.31 ppm (s)) of xylogranatin M (**8**) to the carbonyl carbon atom of this acetoxy group. Treatment of xylogranatin I (**4**) with acetic anhydride in pyridine, followed by methylation of the acetylated product with (trimethylsilyl)diazomethane, gave xylogranatin M (**8**) (Scheme 3). The absolute configuration of C3 in **8** was determined to be the same as in **4** by NOE interactions that were observed from H3 to H5. Therefore, the structure of xylogranatin M (**8**) was identified as the 3-*O*-acetyl-9-methylester analogue of xylogranatin I (**4**).

Similiar 1D and 2D NMR spectroscopy investigations established the structures of xylograntines N–P (**9**–**11**) as seen in Scheme 1 (for more details see the Experimental Section and the Supporting Information).

The molecular formula of xylogranatin Q (**12**) was determined to be $C_{27}H_{30}O_9$ by HR-TOFMS (*m*/*z*: calcd: 521.1788; found: 521.1796 $[M+Na]^+$). The ^1H and ^{13}C NMR spectroscopy data (see Experimental Section and Table 2) indicated the presence of five carbon–carbon double bonds, three carbonyls, and five rings. By detailed analysis of the 2D ^1H-^1H COSY, HSQC, and HMBC spectra of xylogranatin Q (**12**), it was found that this compound could be divided into three substructures (Figure 8a), namely, **12a** (from C9, C11 to 18 and from C20 to C23), **12b** (from C3 to C7, C10, C19, C28, and C29), and **12c** (a furan ring that comprises C1, C2, C8, and C30). Although **12a** and **12c** were the same as **4a** and **4c** of xylogranatin I (**4**), the substructure **12b** was distinctly different from that of **4b**. The presence of two oxygenated methines C3 ($\delta_H = 4.51$ ppm; $\delta_C = 81.6$ ppm) and C6 ($\delta_H = 4.21$ ppm (s); $\delta_C = 84.3$ ppm (d)) in **12b** was suggested by their ^1H and ^{13}C NMR spectroscopic data. The HMBC correlations between H6/C3 and H3/C6 indicated that these methines were connected by an oxygen bridge. The presence of this oxygen bridge was consistent with the above-described unsaturation analysis of the molecular formula of xylogranatin Q (**12**). From the view of biosynthesis, xylogranatin Q (**12**) should be derived from xylogranatin I (**4**), by oxidation of C6, and subsequent dehydrating ether formation between C3 and C6 to form a tetrahydrofuran ring (see below).

The relative configurations within **12** were established on the basis of the NOESY spectrum. The significant NOE interactions between H3/H6, H3/H30, H3/Me28, H3/Me29, H5/H6, H5/Me19 and Me19/Me28 that were observed in **12** (Figure 8b) indicated the relative orientation of substructures **12b** and **12c** to each other as shown in Figure 8b. Similarly, the interactions between H17/H12, H17/H15, H17/H22, Me18/H15, Me18/H21, Me18/H30, and H30/H15 suggested that Me18 is α, H17 is β, and therefore that the 17-substituted β-furyl ring is α. Further, the NOE interactions of Me19/H15 and H5/H15 are an additional indication of the spatial proximity of the substructures **12a** and **12b**.

The absolute configuration of **12** was evidenced by CD analysis. The CD spectrum of **12** was taken in methanol of chromatographic grade, and it exhibited two positive and

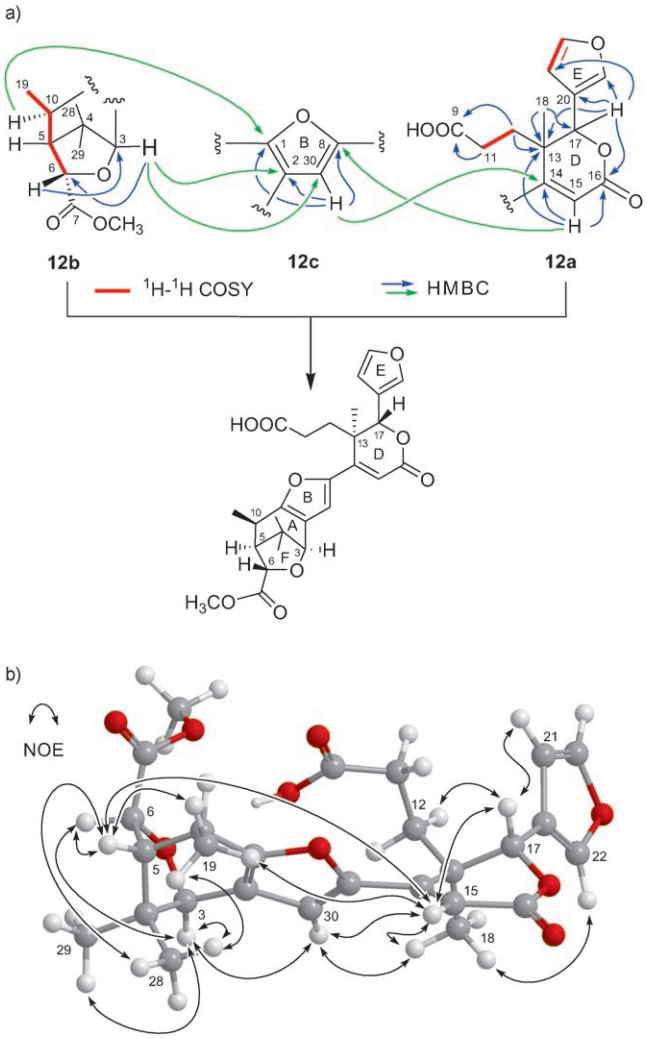

Figure 8. (a) Substructures of xylogranatin Q (**12**) (blue arrows indicate interactions within the fragments, green ones between them). (b) Significant NOE correlations for xylogranatin Q (**12**).

one negative Cotton effects at $\lambda = 219$ ($\Delta\varepsilon = +13.0$), 264 ($+3.2$), and 326 nm ($-3.2$ cm^{2}mol^{-1}), which were similar to those of xylogranatin I (**4**) ($\lambda = 219$ ($\Delta\varepsilon = +8.6$), 264 ($\Delta\varepsilon = +3.4$), and 326 nm ($\Delta\varepsilon = -3.1$ cm^{2}mol^{-1}); see Figure S8 in the Supporting Information). The chromophores in **12** are similiar to those in **4**; ring B is the main chromophore for the southwestern moiety, and ring D and E are the main chromophores for the northeastern part. Despite the fact that **12** has an additional ring (viz., ring F), the chromophore of the southwestern moiety is nearly the same as in **4** and has an almost identical stereochemical orientation, as the substituents at C3 and C5 of ring A in the main conformers of xylogranatin I (**4**) both adopt an axial array, as was also found for ring A of xylogranatin Q (**12**). The only difference is the bond between O3 and C6 in **12**. Although this bond generates an additional stereogenic center in the southwestern moiety, this center is far away from the main chromophore and thus should not give an additional Cotton effect in the CD spectrum. For these reasons, the nearly

identical CD spectra of **12** and **4** indicate that **12** should indeed have the same absolute configuration as **4**, and the configuration of the additional stereocenter at C6 can be determined from the NOE investigations.

Xylogranatin R (**13**) was isolated as an amorphous powder. Its molecular formula was determined to be $C_{27}H_{32}O_9$ by HR-TOFMS (*m*/*z*: calcd: 523.1944; found: 523.1956 $[M+Na]^+$). The ^1H and ^{13}C NMR spectroscopic data (Table 2 and Experimental Section) indicate that the molecule has four carbon–carbon double bonds, five carbonyls, and three rings. By a detailed analysis of the 2D ^1H-^1H COSY, HSQC, and HMBC spectra of xylogranatin R (**13**), it was found that **13** could be divided into three substructures (Figure 9), namely, **13a** (from C9, C11 to 18 and

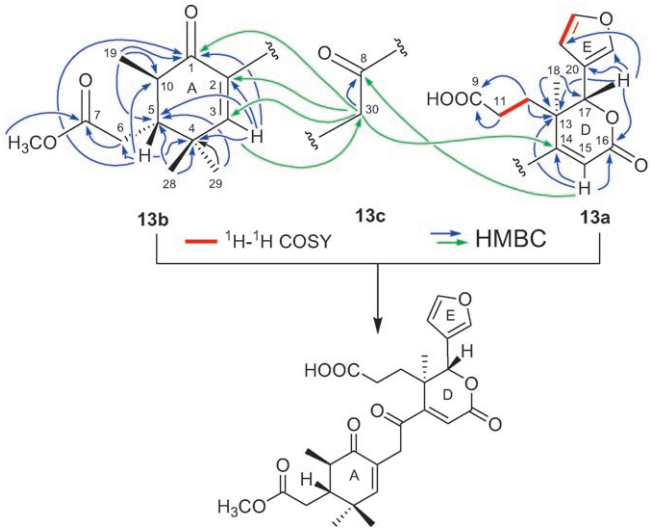

Figure 9. Partial structures, ^1H-^1H COSY and HMBC correlations that were used to establish the structure of xylogranatin R (**13**) (blue arrows indicate interactions within the fragments, green ones indicate interactions between the fragments).

from C20 to C23), **13b** (from C1 to C7, C10, C19, C28, and C29) and **13c** (from C8 and C30), among which **13a** and **13b** were the same as **12a** and the corresponding substructure of xylogranatin C,[20] respectively. The substructure **13b** could be assembled by starting from a proton spin system, H6–H5–H10–$H_3$19, which was deduced from ^1H-^1H COSY correlations. HMBC cross-peaks from H6 to the ester carbon of a methoxycarbonyl group (δ_H=3.70 ppm (s); δ_C= 52.0 (q), 173.6 ppm (s)) connected C6 with this terminal group. A proton singlet of an olefinic methine (C3) resonance at δ_H=6.54 ppm and two methyl singlet resonances at δ_H=1.19 (Me29) and 1.11 ppm (Me28), which exhibit HMBC correlations to a quaternary carbon atom (C4) and C5 of the above-described proton spin system suggested that the quaternary-carbon atom (C4) that bears two methyl groups was situated between C3 and C5. On the other hand, HMBC cross-peaks from the olefinic proton, H10 and Me19, to a conjugated ketone (δ_C=200.5 ppm (s)) indicated that this ketone was situated between C2 and C10. Based on the above observations, it was concluded that the carbon atoms C1–C5 and C10 comprised a cyclohex-2-enone ring. Together this gave the substructure **13b**, which was the same as that in xylogranatin C,[20], which was isolated from the seeds of the same plant. The remaining fragment, **13c**, was assembled as a methylene connected with a ketone on the basis of the NMR spectroscopic data: δ_H=3.45 (d, J= 16.8 Hz), 3.75 ppm (d, J=16.8 Hz); δ_C=41.4 (t), 197.8 ppm (s) (Tables 2 and Experimental Section). The connections between the above fragments were elucidated by HMBC correlations between the protons and carbon atoms that belong to different substructures. The observed HMBC cross-peaks H30/C1, H30/C2, H30/C3, and H3/C30 connected the substructures **13b** and **13c** through the carbon–carbon bond of C2−C30, while the HMBC correlations $H_2$30/C14 and H15/C8, linked fragments **13c** and **13a** together through that of C8−C14 (Figure 9).

The relative stereostructure of **13** was established by analysis of its NOESY spectrum. The significant NOE interactions, H17/H12a, H17/H12b, H17/H15, H17/H22, Me18/H21, and Me18/H15 suggested a 17β-H and a 18α-Me orientation. The correlations H30b/H3, H30b/H5, H30b/Me19, and Me19/Me28 indicated that H5 and Me19 of substructures **13b** are β-configured (see Figure S7 in the Supporting Information).

Absolute configuration of xylogranatins F–R (1–13): As mentioned earlier, the absolute stereostructures of xylogranatins F (**1**) and I (**4**) were determined by application of the modified Mosher MTPA ester method coupled with circular dichroism quantum chemical calculations. The successful chemical conversions of **1** to **2** and **3** (Scheme 2), combined with the NOE correlation studies on the stereoarray at C3 in these compounds confirmed that they all possess the same configurations at their chiral centers at C3, C5, C10, C13, and C17, which were determined to be *R*, *S*, *S*, *R*, and *R*, respectively. The configuration at C14 in **3** was deduced as *S* by the NOE interaction from H14 to Me18. That compounds **4**–**11** had the same *R* configurations at C3, 5, 10, 13, and 17, was corroborated by the successful chemical transformations of **4** and **6** to **5**, of **4** to **7** and to **8**, and of **9**–**11** to **8** (Scheme 3). Moreover, the absolute configuration at C2 in the 2-methylbutyryl group of **9** was determined to be *S* by the α_D value of its acid and the *E*-configured double bond in the tigloyl group (2-methylcrotonyl) of **10** was suggested by its NOE correlation studies. Furthermore, the chiral center at C17 of **12** was identified as the same as that of **4**–**11** by analysis of its CD spectrum (see Figure S8 in the Supporting Information), while others, including C3, C5, C6, C10, and C13 were suggested to be *R*, *S*, *S*, *R*, and *R*, respectively, by their NOE interactions. Although some of the NOE interactions were quite weak and not as significant as in the case of the xylogranatins **F**–**P**, nonetheless, this should be the most probable stereochemical array due to the joint biogenetic origin of **12** compared to those of **4**–**11**. Likewise, for biosynthetic reasons, we anticipate that in the case of xylogranatin R (**13**) the stereogenic centers at C5, C6, C13, and C17 should have the *R* configuration.

Possible joint biosynthetic origin of xylogranatins F–R (1–13): Xylogranatins F–R (**1**–**13**) constitute a novel type of natural products that consist of 26 carbon atoms in their skeletons. Among them, the xylogranatins F–Q (**1**–**12**) belong to two subclasses of tetranortriterpenoids, one of which, compounds (**1**–**3**), comprises a pyridine as the B-ring of tetranortriterpenoid, while the other subclass (**4**–**12**) contains a central furan core. A plausible biogenetic pathway for xylogranatins F–Q (**1**–**12**), with xylogranatin R (**13**) as a key biosynthetic intermediate, is proposed in Scheme 4. The biogenetic origin of them might be a mexicanolide,[4] the retro-aldol cleavage of the C9−C10 bond of which could lead to the opening of its B ring, thus generating xylogranatin C. Further cleavage of the C8−C9 bond of xylogranatin C, with loss of its 30-acetoxy group, would lead to the key intermediate, xylogranatin R (**13**), which, as a 1,4-diketone could cyclize to produce a hypothetical heterocyclic intermediate, **int A**, and then aromatize to generate the furan derivative xylogranatin I (**4**). Different substitution reactions at C3 and at the 9-carboxylate group of xylogranatin I (**4**) would produce xylogranatins J–P (**5**–**11**). While oxidation of C6 of xylogranatin I (**4**) and cyclic ether formation with C3 could generate the complex structure of xylogranatin Q (**12**), oxidation at C10 with γ-lactonization and transformation of the C9 carboxyl group into a nitrile function would result in the pentacyclic compound **int B**. By starting from this nitrogen-containing compound, the central pyridine ring of **1**–**3** might be generated by two possible subpathways: either through a direct hetero-Diels–Alder-related ring closure to give **int D** and subsequent hydrogenation to give **int F**, or by reduction, followed by the Diels–Alder ring closure at the level of the imine **int C** to give **int E**, and final elimination of water via **int F**, thus completing the biosynthesis of xylogranatin F (**1**), which could then be transformed to xylogranatins G (**2**) and H (**3**) by acetylation of its 3-OH group and hydrogenation of its C14–C15 double bond, respectively.

Antifeedant activity of xylogranatins: The new compounds, xylogranatins C and D[20] (not shown), F–G (**1**, **2**), I–K (**4**–**6**), and P–R (**12**, **13**), were tested for their antifeedant activities by using a conventional leaf disk method against the third instar larvae of *Mythimna separata* (Walker) (Table 3).[29] Compounds **1**, **2**, **4**, **13**, and xylogranatin D exhibited marked antifeedant activity at a concentration of 1 mg mL^{-1}. The antifeedant rates of these compounds at the exposure times of 24, 48, and 72 h were over 50% in all cases. Among the above-mentioned five compounds, **2**, **4** and **13** proved to be the most potent ones; they provided antifeedant rates of over 70% at the exposure time of 24 h. The most potent compound tested was xylogranatin G (**2**). Its antifeedant rate was 74–80% and was stable at different exposure times, but those of **4** and **13** decreased with longer exposure times. As shown in Table 3, the antifeedant activity of xylogranatin G (**2**) is much stronger than that of one standard, podophyllotoxin,[30,31] but it is slightly weaker than that of another standard, toosendanin.[32] A detailed study showed that its AFC_{50} (concentration for 50% antifeedant activity) values at 24 and 48 h were 0.31 and 0.30 mg mL^{-1}, respectively.

Table 3. Antifeedant bioassay results for xylogranatins C–D, F–G (**1**–**2**), I–K (**4**–**6**), and P–R (**12**–**13**).

Compound	Concn [mg mL^{-1}]	Antifeedant rates at different exposure time (mean ± SD %)		
		24 h	48 h	72 h
1	1.0	50.0 ± 5.8	55.2 ± 7.1	57.7 ± 10.2
2	1.0	74.1 ± 8.7	79.9 ± 6.3	73.8 ± 3.5
4	1.0	74.5 ± 4.2	59.0 ± 2.5	43.3 ± 2.3
5	1.0	38.3 ± 3.1	45.4 ± 3.7	34.9 ± 2.7
6	1.0	6.4 ± 4.8	28.5 ± 8.8	32.3 ± 3.6
12	1.0	45.0 ± 4.0	58.5 ± 8.1	44.2 ± 4.4
13	1.0	70.6 ± 2.4	58.6 ± 5.3	47.5 ± 7.8
xylogranatin C	1.0	48.3 ± 10.3	46.9 ± 2.1	51.5 ± 5.2
xylogranatin D	1.0	53.3 ± 7.4	57.3 ± 4.7	55.7 ± 9.3
toosendanin[a]	1.0	88.3 ± 1.2	95.6 ± 2.3	100.0
podophyllotoxin[a]	1.0	53.2 ± 2.7	57.2 ± 4.7	68.4 ± 3.3

[a] Antifeedant standards.

Xylogranatin G (**2**) is the 3-*O*-acetyl derivative of xylogranatin F (**1**). The introduction of this *O*-acetyl group at the 3-hydroxyl of xylogranatin F (**1**) enhanced the antifeedant rate significantly (16 to 25%) (Table 3). Thus, the SAR study on the C3 analogues of xylogranatin F (**1**) might generate even more potent antifeedant leads. The synthesis of these analogues for antifeedant evaluation is in progress.

Conclusion

Xylogranatins F–R, from the seeds of the Chinese mangrove, *Xylocarpus granatum*, were isolated and identified as a class of limonoids with a new carbon skeleton. Xylogranatins F–Q are the first aromatic B-ring limonoids to be found in nature. They belong to two new subclasses, one comprises a pyridine portion as the B ring of tetranortriterpenoid and the other one contains a central furan ring. Xylogranatins C and R are key biosynthetic intermediates, while xylogranatin D clearly is an artifact. The structures of these limonoids suggest a new biogenetic pathway to tetranortriterpenoids. Xylogranatins F, G and R exhibited pronounced antifeedant activity against the third instar larvae of *Mythimna separata* (Walker) at a concentration of 1 mg mL^{-1}. The most potent compound tested was xylogranatin G. Its AFC_{50} (concentration for 50% antifeedant activity) values at 24 and 48 h were 0.31 and 0.30 mg mL^{-1}, respectively. This study demonstrates that *X. granatum* is a rewarding new source for the production of limonoids with novel carbon frameworks.

Experimental Section

General procedures: Optical rotations were recorded on a Polaptronic HNQW5 automatic high-resolution polarimeter (Schmidt & Haensch, Berlin, Germany) and on a J-715 spectropolarimeter (JASCO, Gross-Umstadt, Germany) at room temperature by using a 0.1 cm standard cell

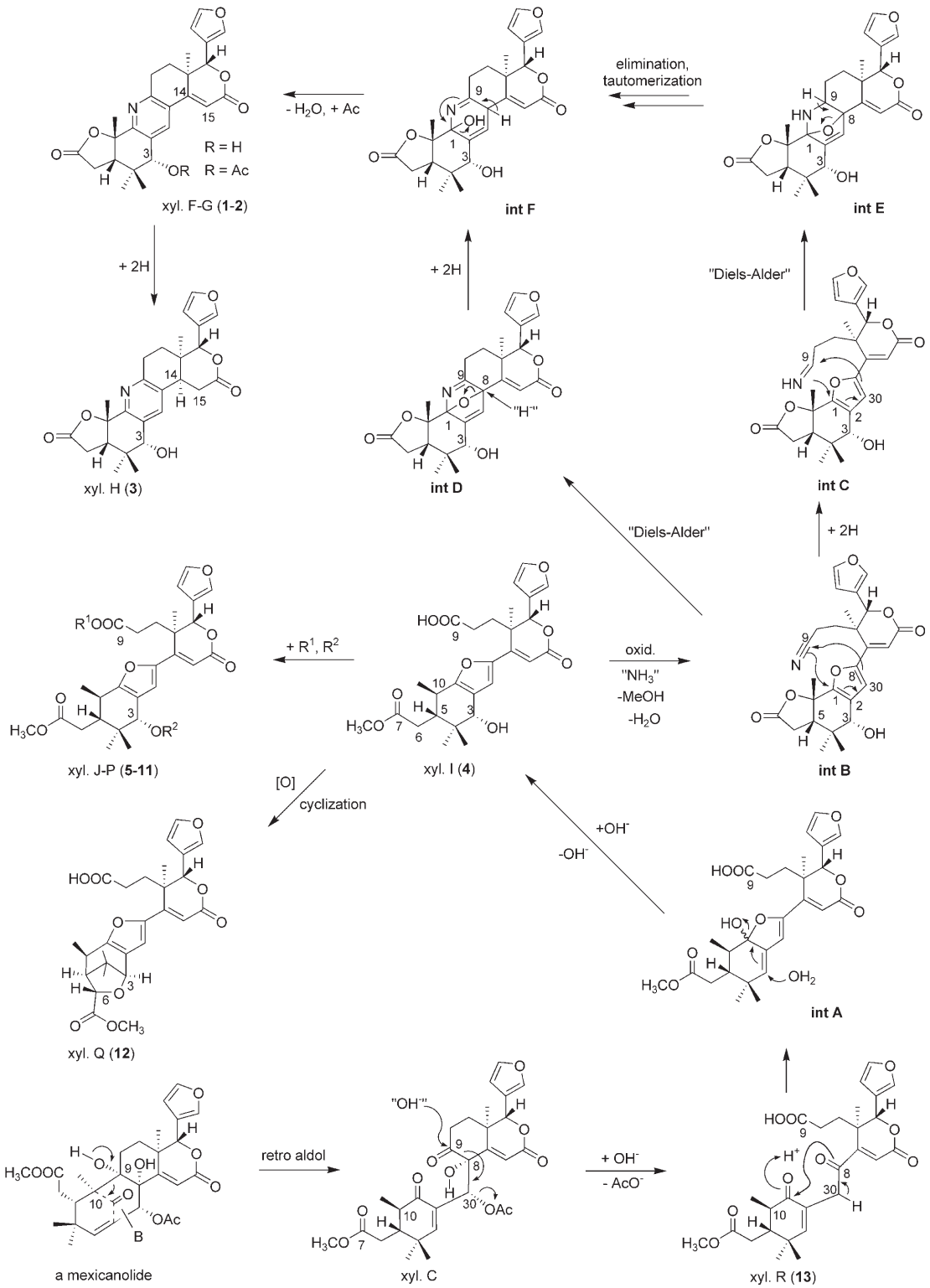

Scheme 4. Proposed biogenetic pathway to xylogranatins F–R (xyl = xylogranatin).

and spectrophotometric grade MeOH, and are reported in $\Delta\varepsilon$ values (cm^2mol^{-1}) at the given wavelength λ (nm). UV spectra were obtained on a Beckman DU-640 UV spectrophotometer. IR spectra were recorded on a Bruker Vertex-70 FTIR spectrophotometer. ESI-MS and TOF-MS spectra were obtained on Bruker APEX II and BiflexIII MALDI-TOF mass spectrometers, respectively (positive or negative mode). NMR spectra were recorded in $CDCl_3$ or [D_4]methanol by using a Bruker AV-500 spectrometer (500 MHz for ^{1}H NMR and 125 MHz for ^{13}C NMR spectra)

with tetramethylsilane as the internal standard. Preparative HPLC was carried out on ODS columns (250×10 mm i.d., YMC) with a Waters 996 photodiode array detector. For column chromatography, silica gel (200–300 mesh) (Qingdao Mar. Chem. Ind.) was used. (*R*)-, (*S*)-MTPACl and (dimethylamino)pyridine (DMAP) were purchased from Sigma–Aldrich.

Plant material: Four batches of the seeds of *Xylocarpus granatum* were collected in October and November 2005, and in January and March 2006 from the Hainan Island (Southern China). The identification of the plant was performed by Prof. Yongshui Lin, Laboratory of Marine Biology, South China Sea Institute of Oceanology, Chinese Academy of Sciences. Voucher samples (nos. GKLMMM-002–4 to GKLMMM-002–7) are maintained in the Herbarium of the South China Sea Institute of Oceanology.

Extraction and isolation: Four batches of the dried seeds (4, 6, 6, and 8 kg, each) of *X. granatum* were crushed and extracted three times with 95% ethanol at room temperature. The extract was concentrated and partitioned between water and petroleum ether. Then the aqueous layer was further extracted with ethyl acetate and concentrated to give a brown gum, which was subjected to silica-gel chromatography (chloroform/methanol 100:0 to 2:1). The fractions that were eluted with chloroform/methanol (25:1 to 15:1) were combined and purified by preparative HPLC (YMC-Pack ODS-5 A, 250×20 mm i.d., acetonitrile/water 30:70 to 45:55) to yield xylogranatins F (**1**, 20 mg), G (**2**, 22 mg), H (**3**, 4 mg), I (**4**, 40 mg), J (**5**, 8 mg), K (**6**, 20 mg), L (**7**, 6 mg), M (**8**, 3 mg), N (**9**, 6 mg), O (**10**, 7 mg), P (**11**, 6 mg), Q (**12**, 35 mg), R (**13**, 12 mg), and C[20] (60 mg). Additionally, xylogranatin C was stored for two weeks dissolved in methanol at room temperature; after this time, it was purified by HPLC to afford xylogranatin D[20] (35 mg).

Xylogranatin F (1): Amorphous powder, $[\alpha]_D^{25}=+254$ ($c=0.21$ in MeCN); ^{1}H and ^{13}C NMR (see Table 1); IR (film): $\tilde{\nu}=3420$, 2970, 1772, 1712, 1595, 1440, 1365, 1239, 1161, 1129, 1061, 1027, 942, 875, 697, 602 cm^{-1}; UV (MeOH): λ_{max} (logε) = 210 (4.23), 268 (4.01), 310 nm (4.07); HR-TOFMS: *m*/*z*: calcd for $C_{26}H_{27}NO_6Na$: 472.1736 $[M+Na]^+$; found: 472.1724.

Xylogranatin G (2): Amorphous powder, $[\alpha]_D^{25}$ +105 ($c=0.15$ in MeCN); ^{1}H and ^{13}C NMR (see Table 1); IR (film): $\tilde{\nu}=3447$, 2972, 1776, 1726, 1596, 1440, 1373, 1233, 1160, 1082, 1062, 1023, 937, 875, 697, 605 cm^{-1}; UV (MeOH): λ_{max} (logε)=208 (4.21), 270 (3.89), 310 nm (3.96); HR-TOFMS: *m*/*z*: calcd for $C_{28}H_{29}NO_7$: 491.1944 $[M]^+$; found: 491.1947.

Xylogranatin H (3): Amorphous powder, $[\alpha]_D^{25}=+14$ ($c=0.12$ in MeCN); ^{1}H and ^{13}C NMR (see Table 1); IR (film): $\tilde{\nu}=3447$, 2933, 1736, 1632, 1384, 1238, 1163, 1027, 944, 875, 602 cm^{-1}; UV (MeOH): λ_{max} (logε)=217 (4.03), 280 nm (4.01); HR-TOFMS: *m*/*z*: calcd for $C_{26}H_{29}NO_6Na$: 474.1893 $[M+Na]^+$; found: 474.1884.

Xylogranatin I (4): Amorphous powder, $[\alpha]_D^{25}=-20$ ($c=0.20$ in MeOH); ^{1}H NMR (CD_3OD): $\delta=0.76$ (s, H28), 1.05 (s, H29), 1.27 (s, H18), 1.36 (d, $J=6.7$ Hz, H19), 1.92 (dt, $J=14.5$, 4.0 Hz, H12a), 2.17 (dt, $J=16.0$, 4.0 Hz, H11a), 2.32 (m, H5), 2.35 (m, H6a), 2.57 (m, H6b), 2.38 (m, H12b), 2.47 (dt, $J=16.0$, 5.0 Hz, H11b), 2.60 (m, H10), 3.70 (s, 7-OCH_3), 4.05 (s, H3), 5.52 (s, H17), 6.39 (s, H15), 6.53 (brs, H22), 7.08 (s, H30), 7.67 (brs, H21), 7.53 ppm (brs, H23); ^{13}C NMR (see Table 2); IR (film): $\tilde{\nu}=3436$, 2970, 1631, 1582, 1384, 1027, 874, 603 cm^{-1}; UV (MeOH): λ_{max} (logε)=213 (4.09), 336 nm (4.12); HR-TOFMS: *m*/*z*: calcd for $C_{27}H_{32}O_9$: 500.2046 $[M]^+$; found: 500.2052.

Xylogranatin J (5): Amorphous powder, $[\alpha]_D^{25}=-73$ ($c=0.10$ in MeOH); ^{1}H NMR (CD_4OD): $\delta=0.77$ (s, H28), 1.08 (s, H29), 1.31 (s, H18), 1.34 (d, $J=6.7$ Hz, H19), 1.95 (dt, $J=14.5$, 4.0 Hz, H12a), 2.20 (dt, $J=16.0$, 4.0 Hz, H11a), 2.37 (m, H6a), 2.38 (m, H5), 2.40 (m, H12b), 2.53 (dt, $J=$ 16.0, 5.0 Hz, H11b), 2.58 (m, H6b), 2.59 (m, H10), 3.38 ppm (s, 3-OCH_3), 3.63 (s, 9-OCH_3), 3.66 (s, H3), 3.71 (s, 7-OCH_3), 5.54 (s, H17), 6.41 (s, H15), 6.56 (brs, H22), 7.16 (s, H30), 7.56 (brs, H23), 7.70 ppm (brs, H21); ^{13}C NMR (see Table 2); IR (film): $\tilde{\nu}=3435$, 2932, 2375, 1631, 1581, 1406, 1385, 1027, 832, 620 cm^{-1}; UV (MeOH): λ_{max} (logε)=212 (4.12), 335 nm (4.13); HRTOF-MS *m*/*z*: calcd for $C_{29}H_{36}O_9Na$: 551.2257 $[M+Na]^+$; found: 551.2237.

Xylogranatin K (6): Amorphous powder, $[\alpha]_D^{25}=-31$ ($c=0.13$ in MeOH); ^{1}H NMR (CD_3OD): $\delta=0.74$ (s, H28), 1.05 (s, H29), 1.28 (s, H18), 1.32 (d, $J=6.7$ Hz, H19), 1.89 (dt, $J=14.5$, 4.0 Hz, H12a), 2.14 (dt, $J=16.0$, 4.0, H11a), 2.33 (m, H6a), 2.36 (m, H5), 2.38 (m, H12b), 2.46 (dt, $J=16.0$, 5.0 Hz, H11b), 2.54 (m, H6b), 2.56 (m, H10), 3.35 (s, 3-OCH_3), 3.63 (s, H3), 3.68 (s, 7-OCH_3), 5.52 (s, H17), 6.39 (s, H15), 6.54 (brs, H22), 7.14 (s, H30), 7.53 (brs, H23), 7.67 ppm (brs, H21); ^{13}C NMR (see Table 2); IR (film): $\tilde{\nu}=3434$, 2939, 2374, 1710, 1631, 1583, 1385, 1270, 1164, 1089, 1028, 874, 804, 603 cm^{-1}; UV (MeOH): λ_{max} (logε)=212 (4.09), 335 nm (4.19); HRTOF-MS: *m*/*z*: calcd for $C_{28}H_{34}O_9Na$: 537.2101; found: 537.2112 $[M+Na]^+$.

Xylogranatin L (7): Amorphous powder, $[\alpha]_D^{25}=-37$ ($c=0.12$ in MeOH); ^{1}H NMR (CD_3OD): $\delta=0.77$ (s, H28), 1.09 (s, H29), 1.20 (t, $J=7.0$ Hz, 3-OCH$_2$CH_3), 1.30 (s, H18), 1.36 (d, $J=6.7$ Hz, H19), 1.93 (dt, $J=14.5$, 4.0 Hz, H12a), 2.16 (dt, $J=16.0$, 4.0 Hz, H11a), 2.36 (m, H6a), 2.39 (m, H12b), 2.40 (m, H5), 2.47 (dt, $J=16.0$, 5.0 Hz, H11b), 2.57 (m, H6b), 2.60 (m, H10), 3.52 (m, 3-OCH_2CH$_3$), 3.67 (m, 3-OCH_2CH$_3$), 3.71 (s, 7-OCH_3), 3.76 (s, H3), 5.55 (s, H17), 6.41 (s, H15), 6.57 (brs, H22), 7.13 (s, H30), 7.56 (brs, H23), 7.70 ppm (brs, H21); ^{13}C NMR (see Table 2); IR (film): $\tilde{\nu}=3435$, 2973, 2376, 1715, 1632, 1583, 1385, 1271, 1165, 1086, 1027, 875, 802, 603 cm^{-1}; UV (MeOH): λ_{max} (logε)=212 (4.15), 336 nm (4.21); HRTOF-MS: *m*/*z*: calcd for $C_{29}H_{36}O_9Na$: 551.2257 $[M+Na]^+$; found: 551.2268.

Xylogranatin M (8): Amorphous powder, $[\alpha]_D^{25}=-52$ ($c=0.15$ in MeOH); ^{1}H NMR (CD_3OD): $\delta=0.87$ (s, H28), 1.04 (s, H29), 1.27 (s, H18), 1.36 (d, $J=6.7$ Hz, H19), 1.94 (dt, $J=14.5$, 4.0 Hz, H12a), 2.07 (s, 3-OCOCH_3), 2.19 (dt, $J=16.0$, 4.0 Hz, H11a), 2.35 (m, H12b), 2.40 (m, H5), 2.43 (m, H6a), 2.52 (dt, $J=16.0$, 5.0 Hz, H11b), 2.62 (m, H6b), 2.65 (m, H10), 3.64 (s, 9-OCH_3), 3.73 (s, 7-OCH_3), 5.31 (s, H3), 5.53 (s, H17), 6.40 (s, H15), 6.55 (brs, H22), 7.01 (s, H30), 7.56 (brs, H23), 7.69 ppm (brs, H21); ^{13}C NMR (see Table 2); IR (film): $\tilde{\nu}=3435$, 2971, 2375, 1732, 1631, 1588, 1384, 1242, 1166, 1129, 1024, 875, 806, 604 cm^{-1}; UV (MeOH): λ_{max} (logε)=212 (4.10), 336 nm (4.11); HR-TOFMS: *m*/*z*: calcd for $C_{30}H_{36}O_{10}Na$: 579.2206 $[M+Na]^+$; found: 579.2214.

Xylogranatin N (9): Amorphous powder, $[\alpha]_D^{25}=-41$ ($c=0.15$ in MeOH); ^{1}H NMR (CD_3OD): $\delta=0.88$ (s, H28), 1.04 (s, H29), 1.25 (s, H18), 1.38 (d, $J=6.7$ Hz, H19), 1.92 (m, H12a), 2.14 (m, H11a), 2.34 (m, H12b), 2.42 (m, H5), 2.43 (m, H11b), 2.45 (m, H6a), 2.62 (m, H6b), 2.65 (m, H10), 3.73 (s, 7-OCH_3), 5.29 (s, H3), 5.53 (s, H17), 6.39 (s, H15), 6.54 (brs, H22), 7.00 (s, H30), 7.54 (brs, H23), 7.69 ppm (brs, H21); 3-*O*-(2*S*)methylbutyryl: 0.86 (t, $J=7.4$ Hz, H4′), 1.13 (d, $J=7.0$ Hz, H5′), 1.50 (m, H3′), 1.65 (m, H3′), 2.38 ppm (m, H2′); ^{13}C NMR (see Table 2); UV (MeOH): λ_{max} (logε)=212 (4.06), 335 nm (4.11); IR (film): $\tilde{\nu}=3434$, 2970, 2375, 1721, 1631, 1587, 1384, 1267, 1186, 1027, 875, 807, 603 cm^{-1}; HR-TOFMS: *m*/*z*: calcd for $C_{32}H_{40}O_{10}Na$: 607.2519 $[M+Na]^+$; found: 607.2531.

Xylogranatin O (10): Amorphous powder, $[\alpha]_D^{25}=-28$ ($c=0.11$ in MeOH); ^{1}H NMR (CD_3OD): $\delta=0.89$ (s, H28), 1.03 (s, H29), 1.27 (s, H18), 1.39 (d, $J=6.7$ Hz, H19), 1.93 (m, H12a), 2.14 (m, H11a), 2.34 (m, H12b), 2.45 (m, H11b), 2.46 (m, H6a), 2.50 (m, H5), 2.63 (m, H6b), 2.67 (m, H10), 3.73 (s, 7-OCH_3), 5.33 (s, H3), 5.54 (s, H17), 6.40 (s, H15), 6.56 (brs, H22), 7.04 (s, H30), 7.55 (brs, H23), 7.70 ppm (brs, H21); 3-*O*-tigloyl: 1.83 (d, $J=7.1$ Hz, H4′), 1.85 (s, H5′), 6.89 ppm (q, $J=7.1$ Hz, H3′); ^{13}C NMR (see Table 2); IR (film): $\tilde{\nu}=3435$, 2950, 2375, 1708, 1631, 1385, 1263, 1084, 1023, 875, 806, 603 cm^{-1}; UV (MeOH): λ_{max} (logε)=212 (4.18), 335 nm (4.00); HR-TOFMS: *m*/*z*: calcd for $C_{32}H_{38}O_{10}Na$: 605.2363 $[M+Na]^+$; found: 605.2374.

Xylogranatin P (11): Amorphous powder, $[\alpha]_D^{25}=-36$ ($c=0.11$ in MeOH); ^{1}H NMR (CD_3OD): $\delta=0.87$ (s, H28), 1.04 (s, H29), 1.26 (s, H18), 1.39 (d, $J=6.7$ Hz, H19), 1.95 (m, H12a), 2.13 (m, H11a), 2.33 (m, H12b), 2.36 (m, H11b), 2.44 (m, H5), 2.44 (m, H6a), 2.63 (m, H6b), 2.65 (m, H10), 3.73 (s, 7-OCH_3), 5.29 (s, H3), 5.54 (s, H17), 6.40 (s, H15), 6.56 (brs, H22), 7.01 (s, H30), 7.54 (brs, H23), 7.70 ppm (brs, H21); 3-O-isobutyryl: 1.13 (d, $J=7.0$ Hz, H4′), 1.17 (d, $J=7.0$ Hz, H3′), 2.58 ppm (m, H2′); ^{13}C NMR (see Table 2); IR (film): $\tilde{\nu}=3435$, 2972, 2375, 1631, 1587, 1385, 1160, 1027, 875, 651 cm^{-1}; UV (MeOH): λ_{max} (logε)=212 (4.12), 335 nm (4.16); HR-TOFMS: *m*/*z*: calcd for $C_{31}H_{38}O_{10}Na$: 593.2363 $[M+Na]^+$; found: 593.2373.

Xylogranatin Q (12): Amorphous powder, $[\alpha]_D^{25}=-38$ ($c=0.13$ in MeOH); ^{1}H NMR (CD_3OD): $\delta=1.08$ (s, H28), 1.15 (s, H29), 1.31 (s,

H18), 1.51 (d, $J=7.4$ Hz, H19), 1.90 (m, H12a), 2.11 (m, H11a), 2.40 (m, H12b), 2.49 (m, H11b), 2.52 (s, H5), 3.24 (q, $J=7.4$ Hz, H10), 3.79 (s, 7-OCH_3), 4.21 (s, H6), 4.51 (s, H3), 5.56 (s, H17), 6.40 (s, H15), 6.57 (brs, H22), 7.09 (s, H30), 7.56 (brs, H23), 7.71 ppm (brs, H21); ^{13}C NMR (see Table 2); IR (film): $\tilde{\nu}=3438$, 2952, 1714, 1631, 1506, 1375, 1262, 1165, 1126, 1051, 1032, 875, 805, 603 cm^{-1}; UV (MeOH): λ_{max} (logε) = 213 (4.13), 336 nm (4.27); HR-TOFMS: m/z: calcd for $C_{27}H_{30}O_9Na$: 521.1788 $[M+Na]^+$; found: 521.1796.

Xylogranatin R (13): Amorphous powder, $[\alpha]_D^{25}=+10$ ($c=0.14$ in MeOH); ^{1}H NMR ($CDCl_3$): $\delta=1.08$ (d, $J=6.5$ Hz, H19), 1.11 (s, H28), 1.19 (s, H29), 1.21 (s, H18), 1.79 (m, H12a), 2.33 (m, H6a), 2.36 (m, H12b), 2.37 (m, H5), 2.40 (m, H11a), 2.40 (m, H11b), 2.45 (m, H10), 2.50 (d, $J=16.0$ Hz, H6b), 3.45 (d, $J=16.8$ Hz, H30a), 3.70 (s, 7-OCH_3), 3.75 (d, $J=16.8$ Hz, H30b), 5.38 (s, H17), 6.47 (brs, H22), 6.54 (s, H3), 6.68 (s, H15), 7.46 (brs, H23), 7.55 ppm (brs, H21); ^{13}C NMR (see Table 2); IR (film): $\tilde{\nu}=3435$, 2954, 2375, 1729, 1680, 1381, 1161, 1084, 1032, 875, 603 cm^{-1}; UV (MeOH): λ_{max} (logε) = 216 (4.03), 232 nm (3.99); HR-TOFMS: m/z: calcd for $C_{27}H_{32}O_9Na$: 523.1944; found: 523.1956 $[M+Na]^+$.

Mosher's MTPA esters 1s/1r and 3s/3r: Xylogranatin F (**1**) (2 mg) was treated with (*R*)-MTPACl (10 μL) and DMAP (1 mg) in dried pyridine (0.5 mL) at room temperature for 5 h. The reaction mixture was concentrated and purified by RP-HPLC (YMC-Pack ODS S-5μ, 250×10 mm i.d.) with aqueous acetonitrile to afford the (*S*)-MTPA ester **1s**. The (*S*)-MTPA ester **3s** and (*R*)-MTPA esters **1r** and **3r** were prepared in the same way.

Ester 1s: Amorphous powder; ^{1}H NMR ($CDCl_3$): $\delta=0.79$ (s, 3H, $H_3$29), 1.05 (s, 3H, $H_3$28), 1.15 (s, 3H, $H_3$18), 1.62 (s, 3H, $H_3$19), 1.77 (dt, $J=$ 13.5, 5.0 Hz, H12β), 1.89 (dd, $J=13.5$, 4.0 Hz, H12α), 2.55 (dd, $J=18.5$, 1.0 Hz, H6β), 2.75 (d, $J=9.5$ Hz, H5), 2.99 (dd, $J=18.5$, 9.5 Hz, H6α), 3.12 (dt, $J=19.0$, 5.0 Hz, H11α), 3.25 (dd, $J=19.0$, 4 Hz, H11β), 5.26 (s, H17), 5.73 (s, H3), 6.52 (brs, H22), 6.58 (s, H15), 7.48 (brs, H23), 7.56 (brs, H21), 8.22 ppm (s, H30); ESI-MS: m/z: 666 $[M+H]^+$, 688 $[M+Na]^+$.

Ester 1r: Amorphous powder; ^{1}H NMR ($CDCl_3$): $\delta=0.78$ (s, 3H, $H_3$29), 1.12 (s, 3H, $H_3$28), 1.15 (s, 3H, $H_3$18), 1.45 (s, 3H, $H_3$19), 1.79 (dt, $J=$ 13.0, 5.5 Hz, H12β), 1.89 (dd, $J=13.0$, 5.5 Hz, H12α), 2.53 (dd, $J=18.0$, 1.0 Hz, H6β), 2.73 (d, $J=9.5$ Hz, H5), 2.97(dd, $J=18.0$, 9.5 Hz, H6α), 3.12 (dt, $J=18.5$, 5.0 Hz, H11α), 3.20 (dd, $J=18.5$, 5.5 Hz, H11β), 5.28 (s, H17), 5.64 (s, H3), 6.52 (brs, H22), 6.63 (s, H15), 7.48 (brs, H23), 7.56 (brs, H21), 8.26 ppm (s, H30); ESI-MS: m/z: 666 $[M+H]^+$.

Ester 3s: Amorphous powder; ^{1}H NMR (CD_3OD): $\delta=0.76$ (s, 3H, H29), 1.04 (s, 3H, H18), 1.08 (s, 3H, H28), 1.61 (s, 3H, H19), 1.76 (m, H12β), 2.02 (m, H12α), 2.62 (d, $J=18.8$ Hz, H6β), 2.76 (d, $J=9.5$ Hz, H5), 2.78 (dd $J=16.0$, 11.5 Hz, H15β), 2.89 (dd, $J=18.5$, 16.0 Hz, H15α), 2.99 (dd, $J=18.5$, 5.0 Hz, H11α), 3.15 (H11β), 3.18 (H6α), 3.20 (H14), 5.46 (s, H17), 5.94 (s, H3), 6.62 (brs, H22), 7.60 (brs, H23), 7.68 (brs, H21), 7.89 ppm (s, H30); ESI-MS m/z: 668 $[M+H]^+$, 690 $[M+Na]^+$, 706 $[M+K]^+$.

Ester 3r: Amorphous powder; ^{1}H NMR (CD_3OD): $\delta=0.74$ (s, 3H, H29), 1.04 (s, 3H, H18), 1.21 (s, 3H, H28), 1.28 (s, 3H, H19), 1.76 (m, H12β), 2.02 (m, H12α), 2.61 (d, $J=18.8$ Hz, H6β), 2.73 (d, $J=9.5$ Hz, H5), 2.90 (dd, $J=16.0$, 11.5 Hz, H15β), 2.99 (dd, $J=18.5$, 16.0 Hz, H15α), 3.00 (H11α), 3.15 (H11β), 3.16 (H6α), 3.20 (H14), 5.48 (s, H17), 5.82 (s, H3), 6.63 (brs, H22), 7.60 (brs, H23), 7.68 (brs, H21), 7.93 ppm (s, H30); ESI-MS: m/z: 690 $[M+Na]^+$, 706 $[M+K]^+$.

Mosher's MTPA esters 4′s/4′r: Treatment of **4** (3 mg) with (*R*)- and (*S*)-MTPACl (15 μL) in dichloromethane (0.5 mL) with a mixture of diethylamine (0.2 mL), triethylamine (0.2 mL) and DMAP (2 mg) at room temperature for 12 h afforded **4′** (4 mg). Then **4′** (2 mg) was treated with (*R*)-MTPACl (10 μL) and DMAP (1 mg) in dried pyridine (0.5 mL) at room temperature for 5 h. The reaction mixture was concentrated and purified by RP-HPLC (YMC-Pack ODS S-5μ, 250×10 mm i.d.) with aqueous acetonitrile to afford the (*S*)-MTPA ester **4′s**. The (*R*)-MTPA ester **4′r** was prepared in the same way.

Ester 4′: Amorphous powder; ^{1}H NMR ($CDCl_3$): $\delta=0.75$ (s, 3H, $H_3$28), 1.03 (t, $J=7.1$ Hz, 3H, $H_3$1′), 1.07 (t, $J=7.1$ Hz, 3H, $H_3$1′), 1.08 (s, 3H, $H_3$29), 1.27 (s, 3H, $H_3$18), 1.34 (d, $J=6.8$ Hz, 3H, $H_3$19), 2.04 (m, H12b), 2.19 (m, H12a), 2.28–2.33 (4H, overlapped, H5, H6b, H11a, H11b), 2.51–2.55 (2H, overlapped, H6a, H10), 3.15 (m, 2H, $H_2$2′), 3.32 (m, 2H, $H_2$2′), 3.71 (s, 7-OMe), 4.08 (s, H3), 5.36 (s, H17), 6.44 (s, H15), 6.49 (brs, H22), 6.87 (s, H30), 7.41 (brs, H23), 7.54 ppm (brs, H21); ^{13}C NMR ($CDCl_3$): $\delta=158.1$ (C1), 121.3 (C2), 72.4 (C3), 39.1 (C4), 41.3 (C5), 33.5 (C6), 174.0 (C7), 148.3 (C8), 170.6 (C9), 33.3 (C10), 28.0 (C11), 32.5 (C12), 40.7 (C13), 151.3 (C14), 113.4 (C15), 164.6 (C16), 78.3 (C17), 21.3 (C18), 16.2 (C19), 120.5 (C20), 141.7 (C21), 110.1 (C22), 143.2 (C23), 24.3 (C28), 19.7 (C29), 41.9 (C2′), 40.4 (C2′), 14.4 (C1′), 13.1 ppm (C1′).

Ester 4′s: Amorphous powder; ^{1}H NMR (CD_3OD): $\delta=0.89$ (s, 3H, $H_3$28), 0.96 (s, 3H, $H_3$29), 1.05 (t, $J=7.1$ Hz, 3H, $H_3$1′), 1.09 (t, $J=7.1$ Hz, 3H, $H_3$1′), 1.24 (s, 3H, $H_3$18), 1.38 (d, $J=6.8$ Hz, 3H, $H_3$19), 2.22 (m, H12b), 2.29 (m, H12a), 2.37 (m, H5), 2.48 (m, H11b), 2.42 (dd, $J=16.8$, 4.0 Hz, H6b), 2.59 (dd, $J=16.8$, 10.0 Hz, H6a), 2.65 (m, H11a), 2.68 (m, H10), 3.19 (m, 2H, H_2–2′), 3.46 (m, 2H, H_2–2′), 3.66 (s, 7-OMe), 5.53 (s, H3), 5.60 (s, H17), 6.47 (s, H15), 6.55 (brs, H22), 7.09 (s, H30), 7.56 (brs, H23), 7.70 ppm (brs, H21); ESI-MS: m/z: 538 $[M-MTPAOH]^+$, 560 $[M-MTPAOH+Na]^+$, 794 $[M+Na^+]$, 810 $[M+K^+]$.

Ester 4′r: Amorphous powder; ^{1}H NMR (CD_3OD): $\delta=0.88$ (s, 3H, $H_3$28), 1.03 (t, $J=7.1$ Hz, 3H, $H_3$1′), 1.09 (s, 3H, $H_3$29), 1.09 (t, $J=7.1$ Hz, 3H, $H_3$1′), 1.22 (d, $J=6.8$ Hz, 3H, $H_3$19), 1.31 (s, 3H, $H_3$18), 2.01 (m, H12b), 2.25 (m, H12a), 2.32 (m, H5), 2.33 (m, H11b), 2.40 (dd, $J=16.8$, 4.0 Hz, H6b), 2.53 (m, H11a), 2.56 (dd, $J=16.8$, 10.0 Hz, H6a), 2.62 (m, H10), 3.23 (m, 2H, H2′), 3.32 (m, 2H, H2′), 3.68 (s, 7-OMe), 5.50 (s, H3), 5.62 (s, H17), 6.45 (s, H15), 6.57 (brs, H22), 7.12 (s, H30), 7.56 (brs, H23), 7.71 ppm (brs, H21); ESI-MS: m/z: 538 $[M-MTPAOH]^+$, 560 $[M-MTPAOH+Na]^+$, 794 $[M+Na]^+$, 810 $[M+K]^+$.

Antifeedant bioassay: *Mythimna separata* Walker is a serious crop pest in North China. First or second instar larvae of *M. separata* were collected from a maize field in Shaanxi (China) where pesticides had not been applied. These larvae were reared in the laboratory under a controlled photoperiod (12:12 h light/dark), temperature ($T=25\pm2$ °C), relative humidity ($RH=65\%$ ≈80%), and fed daily with maize leaves until they reached the earlier stage of the third instar larvae, when they were used for antifeedant tests. Three groups of ten larvae each were used for the antifeedant test of one compound. The tested compounds were dissolved in acetone at a concentration of 1 mg mL^{-1}. Wafer discs (1 cm diameter, 1 mm thick), which were made from maize leaves were dipped into acetone solutions of each compound for 3 s and air-dried for 5 min. After drying, one disc was placed in a Petri dish with a *M. separata* larva, which had been starved for 2 h. Another disc was added after the first one had been consumed. After 72 h, undipped discs were given to the larvae. Discs that had been treated with acetone alone were used as a control group. If a whole disc was consumed, food consumption was recorded as 1. If only part of a disc was consumed, the food consumption was assessed by estimating the percentage of the consumed leaf surface. After 24 h, 48 h, or 72 h, the antifeedant rates (AR) were calculated by the following index.

$$AR=(C-T)\times100/C$$

in which C is the average consumption by one larva in the control and T in the treatment. The concentration for 50% antifeedant effect (AFC_{50}) was determined by log-probit analysis. All data were treated by log–probit analysis and 95% fiducial limits were calculated.

Computational details: All optimizations were performed with the software package Gaussian 03,[33] by using the DFT functional B3LYP[22] and the basis set 6–31G(d)[23] To identify the found structures as minima frequency calculations were accomplished on the same level of theory. Rotational strength values for the electronic transitions from the ground state to the singly excited states for **1** and **4** were obtained by time dependent (TD) DFT calculations (B3LYP/6–31G(d)) with Gaussian 03. Additionally Grimme's DFT/MRCI[26] approach (configuration selection cutoff = 0.8 E_h)[34] was used to calculate these values for **1**. Single-point SCF calculations of the B3LYP/6–31G(d)-optimized structures with BHLYP/SVP,[27,35] which were needed for the DFT/MRCI calculations, were carried out with Turbomole 5.8.[36] The rotational strength values were summed after a Boltzmann statistical weighting and $\Delta\varepsilon$ values were calculated by forming sums of Gaussian functions centered at the wave-

lengths of the respective electronic transitions and multiplied by the corresponding rotational strengths. The CD spectra that were obtained, were UV-corrected[25] and compared with the experimental ones.

For further experimental details and considerations on the occurrence of the new compounds as genuine natural products, see the Supporting Information.

Acknowledgements

Support for this work from the Important Projects of the Chinese Academy of Sciences (KZCX3-SW-216 and KZCX2-YW-216), the National High Technology Research and Development Program of China (863 Program) (2007 AA09Z407), the Natural Science Foundation of China (20772135), the Natural Science Foundation of Guangdong Province (04100729), the Fonds der Chemischen Industrie (Germany), and the Deutsche Forschungsgemeinschaft (SPP 1152, "Evolution of Metabolic Diversity", SFB 630 "Recognition, Preparation, and Functional Analysis of Agents against Infectious Diseases") is gratefully acknowledged. Mass spectra were provided by the Institute of Chemistry, Chinese Academy of Sciences, and the NMR spectra by the Laboratory of NMR Analysis and Measurement, South China Sea Institute of Oceanology, Chinese Academy of Sciences. G.B and T.B. are grateful for generous allocation of computational time from Dr. R. Koch, University of Oldenburg (Germany).

[1] A. S. Ng, A. G. Fallis, *Can. J. Chem.* **1979**, *57*, 3088–3089.
[2] I. Kubo, I. Miura, K. Nakanishi, *J. Am. Chem. Soc.* **1976**, *98*, 6704–6705.
[3] K. A. Alvi, P. Crews, B. Aalbersberg, R. Prasad, J. Simpson, R. T. Weavers, *Tetrahedron* **1991**, *47*, 8943–8948.
[4] D. A. Mulholland, B. Parel, P. H. Coombes, *Curr. Org. Chem.* **2000**, *4*, 1011–1054.
[5] U. Kokpol, W. Chavasiri, S. Tip-pyang, G. Veerachato, F. L. Zhao, J. Simpson, R. T. Weavers, *Phytochemistry* **1996**, *41*, 903–905.
[6] J. Wu, M. Y. Li, Z. H. Xiao, Y. Zhou, *Z. Naturforsch. B* **2006**, *61*, 1447–1449.
[7] J. Wu, S. Zhang, Q. Xiao, Q. X. Li, J. S. Huang, Z. H. Xiao, L. J. Long, *Z. Naturforsch. B* **2003**, *58*, 1216–1219.
[8] J. Wu, S. Zhang, Q. Xiao, Q. X. Li, J. S. Huang, L. J. Long, L. M. Huang, *Tetrahedron Lett.* **2004**, *45*, 591–593.
[9] J. Wu, Q. Xiao, J. S. Huang, Z. H. Xiao, S. H. Qi, Q. X. Li, S. Zhang, *Org. Lett.* **2004**, *6*, 1841–1844.
[10] J. Wu, Q. Xiao, S. Zhang, X. Li, Z. H. Xiao, H. X. Ding, Q. X. Li, *Tetrahedron* **2005**, *61*, 8382–8389.
[11] J. Wu, S. Zhang, Y. Song, Z. H. Xiao, Q. Xiao, Q. X. Li, *Z. Naturforsch. B* **2005**, *60*, 1291–1294.
[12] J. Wu, Z. H. Xiao, Y. Song, S. Zhang, Q. Xiao, C. Ma, H. X. Ding, Q. X. Li, *Magn. Reson. Chem.* **2006**, *44*, 87–89.
[13] F. Cheng, Y. Zhou, J. Wu, K. Zou, *Z. Naturforsch. B* **2006**, *61*, 626–628.
[14] Y. Zhou, F. Cheng, J. Wu, K. Zou, *J. Nat. Prod.* **2006**, *69*, 1083–1085.
[15] J. Wu, Q. Xiao, Q. X. Li, *Biochem. Syst. Ecol.* **2006**, *34*, 838–841.
[16] J. Wu, S. Zhang, M. Y. Li, Y. Zhou, Q. Xiao, *Chem. Pharm. Bull.* **2006**, *54*, 1582–1585.
[17] J. Wu, H. X. Ding, M. Y. Li, S. Zhang, *Z. Naturforsch. B* **2007**, *62*, 569–572.
[18] J. X. Cui, Z. W. Deng, J. Li, H. Z. Fu, P. Proksch, W. H. Lin, *Phytochemistry* **2005**, *66*, 2334–2339.
[19] A. D. Roy, R. Kumar, P. Gupta, T. Khaliq, T. Narender, V. Aggarwal, R. Roy, *Magn. Reson. Chem.* **2006**, *44*, 1054–1057.
[20] S. Yin, C. Q. Fan, X. N. Wang, L. P. Lin, J. Ding, J. M. Yue, *Org. Lett.* **2006**, *8*, 4935–4938.
[21] I. Ohtani, T. Kusumi, Y. Kashman, H. Kakisawa, *J. Am. Chem. Soc.* **1991**, *113*, 4092–4096.
[22] a) C. Lee, W. Yang, R. G. Parr, *Phys. Rev. B* **1988**, *37*, 785–789; b) A. D. Becke, *Phys. Rev. A* **1988**, *38*, 3098–3100.
[23] a) P. C. Hariharan, J. A. Pople, *Theor. Chim. Acta* **1973**, *28*, 213–222; b) M. M. Francl, W. J. Pietro, W. J. Hehre, J. S. Binkley, M. S. Gordon, D. J. DeFrees, J. A. Pople, *J. Chem. Phys.* **1982**, *77*, 3654–3665.
[24] Structures that lie energetically higher than 3 kcal mol^{-1} above the energetically lowest structure were found not to contribute to the overall CD curve that was obtained by superposition of the Boltzmann-weighted single spectra.
[25] G. Bringmann, S. Busemann, in *The Quantum Chemical Calculation of CD Spectra: the Absolute Configuration of Chiral Compounds from Natural or Synthetic Origin* (Eds.: P. Schreier, M. Herderich, H.-U. Humpf, W. Schwab), Vieweg, Wiesbaden, **1998**, pp. 195–211.
[26] S. Grimme, M. Waletzke, *J. Chem. Phys.* **1999**, *111*, 5645–5655.
[27] A. Schaefer, H. Horn, R. Ahlrichs, *J. Chem. Phys.* **1992**, *97*, 2571–2577.
[28] J. Wu, Q. Xiao, J. Huang, Z. Xiao, S. Qi, Q. Li, S. Zhang, *Org. Lett.* **2004**, *6*, 1841–1844.
[29] J. Lin, Z. Q. Ma, J. T. Feng, X. Zhang, *Acta Agric. Bor.-Occid. Sin.* **2005**, *14*, 94–97.
[30] R. Gao, X. Tian, X. Zhang, *Acta Univ. Agric. Bor.-Occid.* **2000**, *28*, 8–13.
[31] X. Tian, R. Gao, X. Zhang, *Acta Univ. Agric. Bor.-Occid.* **2000**, *28*, 19–24.
[32] Y. S. Xie, P. G. Fields, M. B. Isman, W. K. Chen, X. Zhang, *J. Stored Prod. Res.* **1995**, *31*, 259–265.
[33] Gaussian 03 (Revision D.01), M. J. Frisch, G. W. Trucks, H. B. Schlegel, G. E. Scuseria, M. A. Robb, J. R. Cheeseman, J. J. A. Montgomery, T. Vreven, K. N. Kudin, J. C. Burant, J. M. Millam, S. S. Iyengar, J. Tomasi, V. Barone, B. Mennucci, M. Cossi, G. Scalmani, N. Rega, G. A. Petersson, H. Nakatsuji, M. Hada, M. Ehara, K. Toyota, R. Fukuda, J. Hasegawa, M. Ishida, T. Nakajima, Y. Honda, O. Kitao, H. Nakai, M. Klene, X. Li, J. E. Knox, H. P. Hratchian, J. B. Cross, V. Bakken, C. Adamo, J. Jaramillo, R. Gomperts, R. E. Stratmann, O. Yazyev, A. J. Austin, R. Cammi, C. Pomelli, J. W. Ochterski, P. Y. Ayala, K. Morokuma, G. A. Voth, P. Salvador, J. J. Dannenberg, V. G. Zakrzewski, S. Dapprich, A. D. Daniels, M. C. Strain, O. Farkas, D. K. Malick, A. D. Rabuck, K. Raghavachari, J. B. Foresman, J. V. Ortiz, Q. Cui, A. G. Baboul, S. Clifford, J. Cioslowski, B. B. Stefanov, G. Liu, A. Liashenko, P. Piskorz, I. Komaromi, R. L. Martin, D. J. Fox, T. Keith, M. A. Al-Laham, C. Y. Peng, A. Nanayakkara, M. Challacombe, P. M. W. Gill, B. Johnson, W. Chen, M. W. Wong, C. Gonzalez, J. A. Pople, Gaussian, Inc., Wallingford CT, **2004**.
[34] C. Diedrich, S. Grimme, *J. Phys. Chem. A* **2003**, *107*, 2524–2539.
[35] A. D. Becke, *J. Chem. Phys.* **1993**, *98*, 1372–1377.
[36] TURBOMOLE (Version 5.8), R. Ahlrichs, M. Bar, H.-P. Baron, R. Bauernschmitt, S. Böcker, N. Crawford, P. Deglmann, M. Ehrig, K. Eichkorn, S. Elliott, F. Furche, F. Haase, M. Häser, H. Horn, C. Hättig, C. Huber, U. Huniar, M. Kattanek, A. Köhn, C. Kölmel, M. Kollwitz, K. May, P. Nava, C. Ochsenfeld, H. Öhm, H. Patzelt, D. Rappoport, O. Rubner, A. Schäfer, U. Schneider, M. Sierka, O. Treutler, B. Unterreiner, M. von Arnim, F. Weigend, P. Weis, H. Weiss, Universität Karlsruhe, Karlsruhe, Germany, **2005**.

Received: May 2, 2007
Revised: September 9, 2007
Published online: November 28, 2007

